



Large-scale ro-ro deck fire suppression tests

Magnus Arvidson

Abstract

Large-scale ro-ro deck fire suppression tests

This report describes a series of large-scale fire suppression tests conducted to simulate a fire on the ro-ro deck of a ship containing heavy goods freight trucks and trailers. Tests were conducted with both a deluge water spray system and a deluge high-pressure water mist system.

The heat release rate (HRR) of the fires and the surface temperatures on two steel screens, positioned to simulate trailers on either sides of the trailer mock-up, were measured.

Parameters such as the water discharge density, the system operating pressure, the nozzle K-factor and whether the fire was fully exposed to the water spray or shielded were varied.

The tests where the fires were fully exposed to the water spray shows that there is a clear relationship between the level of performance and the water application rate. A discharge density of 15 mm/min provided immediate fire suppression, 10 mm/min fire suppression, and 5 mm/min fire control. However, improvements in performance were also documented with a higher system operating pressure and associated smaller water droplets. The high-pressure water mist system provided fire control at a discharge density of 5,8 mm/min. However, tests at 3,75 and 4,6 mm/min, respectively, provided no fire control.

When the fire was shielded from direct water application, the tested systems had a limited effect on the total heat release rate and the associated total energy, as almost all combustible material was consumed. The high-pressure water mist system provided an improved reduction of the convective heat release rate and the associated convective energy as compared to the water spray system.

Key words: Ships, ro-ro decks, sprinklers, water mist, fire, fire suppression.

SP Sveriges Tekniska Forskningsinstitut
SP Technical Research Institute of Sweden

SP Report 2009:29
ISBN 978-91-86319-17-5
ISSN 0284-5172
Borås 2009

Contents

Abstract	3
Contents	4
Preface	6
Summary	7
Sammanfattning	8
1 Background and scope of the project	11
1.1 Background	11
1.2 The scope of the project	13
1.3 The geometrical dimensions of freight trucks	14
1.4 The scope of the tests described in this report	16
2 The fire test set-up	17
2.1 The trailer mock-up	17
2.2 The target screens	19
2.3 The commodity	19
2.4 The potential severity of the fire load	21
2.5 Air velocities around the test set-up	21
3 The fire suppression systems	23
3.1 The system pipe-work	23
3.2 The medium velocity nozzles	24
3.3 The high-pressure water mist nozzles	26
4 Instrumentation and measurements	27
4.1 The Industrial Calorimeter	27
4.2 Surface temperature measurements	28
4.3 System water pressure and water flow rate measurements	29
5 The fire test series and fire test procedures	30
5.1 The fire test series	30
5.2 The fire ignition source	32
5.3 Fire test procedures	32
6 Fire test results	35
6.1 Key parameters	35
6.2 Heat release rate graphs	37
6.3 Temperature measurement graphs	40
7 Discussion	42
7.1 Fire tests without the roof of the trailer mock-up	42
7.2 Fire tests with the roof of the trailer mock-up	44
7.3 Influence of test methodology	47

8	Conclusions	49
8.1	The results from the tests	49
8.2	Practical implications	49
	References	51
	Appendix A	
	Photos: Test 1E(15)	A1
	Photos: Test 2E(10)	A6
	Photos: Test 3E(10)	A12
	Photos: Test 4E(5)	A17
	Photos: Test 5E(HP-3,75)	A27
	Photos: Test 6E(HP-4.6)	A32
	Photos: Test 7E(HP-5.8)	A37
	Photos: Test 8E(10)	A43
	Photos: Test 1S(15)	A51
	Photos: Test 2S(10)	A56
	Photos: Test 3S(10)	A62
	Photos: Test 4S(5)	A68
	Photos: Test 5S(15)	A74
	Photos: Test 6S(HP-5.8)	A80

Preface

This report summarises the outcome of the second phase of the IMPRO-project, “Improved water-based fire suppression and drainage systems for ro-ro vehicle decks”.

The project is sponsored by VINNOVA, the Swedish Governmental Agency for Innovation Systems (project number P31711-1), the Swedish Mercantile Marine Foundation, Brandforsk, the Fire Research Board (project number 401-081) and the Swedish Maritime Administration.

The project was conducted under umbrella project SURSHIP¹.

The work has been conducted in association with a reference group, consisting of the following people:

Anders Kjellberg	Ultra Fog AB
Leif Hanje	Ultra Fog AB
Johan Wikman	Swedish Transport Agency, Maritime Department
Per Fagerlund	ScandiNAOS AB
Bengt Ramne	ScandiNAOS AB
Klas Nylander	Consilium Fire & Gas AB
Thomas Wejdin	Consilium Fire & Gas AB
Harry Robertsson	Stena Shipping AB
Fredrik Efraimsson	Stena Teknik
Agne Karlsson	Stena Teknik
Per Tunell	Wallenius Marine AB
Lars G. Larsson	CCS COBRA Sverige AB
Per Ekberg	VINNOVA
Christer Nordling	The Swedish Mercantile Marine Foundation
Per-Erik Johansson	Brandforsk, the Fire Research Board
Henrik Johansson	TYCO Fire Suppression & Building Products (Sweden AB)

The input and work by Ultra Fog AB for the delivery and installation of the high-pressure water mist system, and of TYCO Fire Suppression & Building Products (Sweden AB) for the delivery of the medium velocity nozzles, is especially acknowledged.

The internal SP project number was BRd 6001.

¹ SURSHIP is a coordinated collaboration involving eight EU-member states. The content and the details in the collaboration are jointly decided. Each participating country provides input to the joint efforts through nationally supported sub-projects, each of which is in line with and considered part of the joint initiative. The collaboration and its sub-projects aims to result in improvements of technologies for quantification of ship’s safety and security performance and the advancement of the decision support systems, rule making and design, with a focus on ROPAX and Cruising ROPAX ships.

Summary

The tests where the fires were fully exposed to the water spray shows that there is a clear relationship between the level of performance and the water application rate. A discharge density of 15 mm/min provided immediate fire suppression, 10 mm/min fire suppression, and 5 mm/min fire control. However, improvements in performance were also documented with a higher system operating pressure and associated smaller water droplets.

The high-pressure water mist system provided fire control at a discharge density of 5,8 mm/min. However, tests at 3,75 and 4,6 mm/min, respectively, provided no fire control.

For the fires, where the fire was shielded from direct water application, the tested systems had a limited effect on the total heat release rate and the associated total energy, as almost all combustible material was consumed in the tests. The most efficient reduction of the convective heat release rate and the associated convective energy was demonstrated with 10 mm/min at a higher system operating pressure.

The high-pressure water mist system provided an improved reduction of the convective heat release rate and the associated convective energy as compared to the water spray system. However, no improved reduction of the total heat release rate and the associated total energy, was documented, i.e., the ability to reduce the actual heat release rate was not improved.

Sammanfattning

Bakgrund

Fordonsutrymmen och ro-ro-lastutrymmen som inte kan tillslutas samt utrymmen av särskild kategori skall enligt kraven i SOLAS kapitel II-2 förses med ett manuellt aktiverat vattenspraysystem. För andra typer av ro-ro lastutrymmen, där personsäkerhetsrisken är lägre - eftersom passagerare inte har tillträde - används normalt koldioxidssystem. Andra typer av inertgassystem, vattensprinklersystem eller lättskumssystem kan också användas men är inte lika vanliga.

Detaljkraven för hur ett vattensprayssystem för fordonsutrymmen och ro-ro-lastutrymmen skall utformas och dimensioneras återfinns i IMO Resolution A.123(V), publicerad år 1967. Några av de detaljkrav som särskilt kan nämnas är att:

- Systemet skall dimensioneras för en vattentäthet om minst 3,5 mm/min för däck med maximalt 2,5 m höjd och för minst 5 mm/min för däck med högre takhöjd.
- Systemet tillåts att delas in i sektioner där varje sektion skall täcka hela fartygets bredd. Undantag från detta krav kan medges om däcket är avdelat i längdled av väggar i "A" klass.
- Varje sektion skall vara minst 20 m lång och systemets pumpar skall ha en kapacitet tillräcklig för antingen hela däcket eller minst två sektioner.
- Sektionsventiler skall vara placerade utanför det skyddade utrymmet.
- Minst en handbrandsläckare skall finnas vid varje utgång från däcket och minst tre strålrör och en mobil skumvagn skall finnas ombord på fartyget.

Under senare år har man från många olika håll ifrågasatt huruvida system i enlighet med Resolution A.123(V) klarar att kontrollera en brand på ett ro-ro däck på ett modernt fartyg med dagens moderna personbilar, turistbussar och tunga lastfordon.

Det engelska sjöfartsverket Maritime and Coastguard Agency (MCA) har nyligen utrett frågan om brandskydd på ro-ro däck, inklusive frågeställningen om den höga brandbelastningen på ro-ro däck och effektiviteten hos nuvarande sprinklersystem. Man drar två intressanta slutsatser i sitt arbete:

1. Att den internationella sjöfartsnäringsen bör koordinera sina insatser och sin kunskap inom detta område.
2. Att ett program med fullskaliga brandförsök genomförs för att öka förståelsen avseende bränder och brandförlopp på ro-ro däck. I ett sådant program borde faktorer såsom typ av brännbart material, antändningskällor, fordonens storlek, fordonens fördelning på däcket, placering av sprinkler, vattentäthet, ventilationsflöden, branddetektion, additiver till vattnet, dränering, etc studeras.

Projektets målsättning

Målsättningen med projektet var att ta fram ett tekniskt underlag för att ersätta kraven i IMO Resolution A.123(V), det vill säga det dokument som idag reglerar hur sprinklersystem för ro-ro däck skall dimensioneras och installeras samt ett tekniskt

underlag för hur ett dräneringssystem för ro-ro däck skall dimensioneras och utformas för att förhindra fria vätskeytor som kan äventyra ett fartygs stabilitet².

Det finns i ett internationellt perspektiv en stor enighet att de sprinklersystem som installeras i fordonsutrymmen och ro-ro-lastutrymmen enligt dagens krav är föråldrade. Mycket har hänt sedan kraven introducerades för drygt 40 år sedan.

Under senare år har alltså även flera internationella projekt berört frågan, men inget av projekten har haft målsättningen att ta fram konkreta rekommendationer för hur mer effektiva sprinkler- och dräneringssystem skall utformas. Målsättningen med detta projekt är att göra just detta.

Projektresultaten skall utgöra ett tekniskt underlag för att ersätta rekommendationerna i IMO Resolution A.123(V). Det sista momentet i projektet är att formulera sådana rekommendationer och att presentera dem för den arbetsgrupp inom IMO som för närvarande jobbar med dessa frågeställningar.

Försök som redovisas i denna rapport

I denna rapport redovisas resultat från fjorton stycken fullskaleförsök där effektiviteten för ett traditionellt vattenspraysystem och ett mer modernt system av typen vattendimma provades i en uppställning som simulerar brand i ett lastbilssläp. Två olika brandscenarier användes, dels ett scenario där branden var fullt exponerad för vattenbegjutning, dels ett scenario där taket över branden förhindrade direkt vattenbegjutning. Det förstnämnda inträffar när kappellet eller taket över ett lastbilssläp brinner av och det sistnämnda om det inte gör det.

Försöken genomfördes med olika vattenflöde (vattentäthet), varierande systemtryck och med olika munstycken. Genom att mäta brandeffekten från branden gick det att få ett mycket bra underlag för att bedöma hur effektiva systemen är.

Försöksresultat

Försöken där branden var fullt exponerad för vattenbegjutning visar att det finns ett klart samband mellan systemets effektivitet och vattentätheten. Vid en vattentäthet motsvarande 15 mm/min ((L/min)/m²) dämpades branden omedelbart efter det att vattenbegjutningen startat. Vid 10 mm/min dämpades också brandeffekten, men inte lika snabbt. Vid den lägsta vattentätheten motsvarande 5 mm/min kontrollerades branden. Resultaten visar även att ett högre systemtryck och mindre vattendroppar förbättrar effektiviteten.

Vattendimmsystemet kontrollerade branden vid en vattentäthet om 5,8 mm/min, men 3,75 mm/min respektive 4,6 mm/min visade sig vara för liten vattenmängd för kontroll av brandförloppet. Högre vattentätheter provades inte.

² Innan projektet hann starta togs denna fråga upp av IMO genom ett gemensamt initiativ från Danmark och Sverige. IMO har behandlat frågan och nya riktlinjer för dränering av ro-ro däck finns publicerade i MSC.1/Circ. 1234. Projektet omfattar därmed inte denna fråga.

För brandscenariot där taket över branden förhindrade direkt vattenbegjutning reducerades inte den totala brandeffekten nämnvärt och i princip allt brännbart material förbrukades. Däremot reducerades den konvektiva brandeffekten, det vill säga de varma brandgaserna kylde. För vattenspraysystemet erhöles den bästa kylningen vid en vattentäthet motsvarande 10 mm/min när vattentrycket ökades.

Vattendimsystemet (5,8 mm/min) reducerade den konvektiva brandeffekten bäst. Däremot reducerades, i likhet med vattenspraysystemet, inte den totala brandeffekten nämnvärt.

1 Background and scope of the project

1.1 Background

Vehicle spaces and ro-ro cargo decks that cannot be closed and special category spaces³ shall, according to the requirements of SOLAS chapter II-2, be fitted with a manually activated water spray system. For other types of ro-ro cargo spaces, where the risk for the people is lower - as passengers do not have access - carbon dioxide system is normally used, although other types of inert gases, water spray or high-expansion foam systems are permitted.

Detailed requirements for the design and installation of water spray systems for vehicle and ro-ro cargo spaces is given in IMO Resolution A.123 (V), published in 1967, see reference [1]. Some detailed requirements that can be mentioned in particular are that:

- The system shall be designed for a water discharge density of at least 3,5 mm/min for decks with a maximum height of 2,5 m height and at least 5 mm/min for decks with higher height.
- The system is allowed to be divided into sections where each section should cover the entire width of the ship. Exemptions from this requirement may be allowed if the deck is separated longitudinally by 'A' class divisions.
- Each section must be at least 20 m long and the system's pumps must have a capacity sufficient for either the entire deck or at least two sections.
- Section valves must be located outside the protected space.
- At least one portable fire extinguisher must be available at each exit from the deck and at least three nozzles and a mobile foam cart shall be available on-board the ship.

One might ask what technical background material has been used to define these detailed requirements? The answer can probably be found in a series of fire trials carried out in Denmark in 1961, see reference [2].

In recent years, questions has been raised as to whether a water spray system in accordance with Resolution A.123 (V) is able to control or suppress a fire on the ro-ro deck of a modern ship with modern cars, coaches and heavy goods vehicles. Two projects funded by the Swedish Fire Research Board (Brandforsk), see SP Report 1997:03 [3] and SP Report 1997:15 [4], discussing this. The latter report describes a large-scale fire test with a layout that represents two trucks, side by side, on a ro-ro deck. The experiment is documented on video [5]. Later, a feasibility study was carried out where the requirements and alternative water-extinguishing systems for cargo were discussed, see reference [6].

The influence of the ventilation conditions has been investigated in model scale. These tests have shown that a fire on a vehicle deck can be very large before it

³ "Special category spaces" are defined as enclosed spaces, situated above or below the bulkhead deck, intended for the carriage of motor vehicles with fuel in their tanks for their own propulsion and to which passengers have access.

becomes ventilation controlled, due to the large volumes associated with ro-ro cargo decks. For decks that typically are 180 m in length, tests and calculations show that a fire can grow to almost 80 MW before the fire becomes ventilation controlled. The average gas temperature is high, of the order of 250°C to 300°C and consequently the temperature and heat radiation directly above the fire can be extremely high. There is an apparent risk for fire spread through the conduction of heat to decks above. As the maximum fire size is a function of the volume of the deck, sectioning of the deck can be an efficient way to limit the size of a fire [7].

The Maritime and Coastguard Agency (MCA) has recently examined the issue of fire protection on ro-ro decks [8] and, e.g., discuss the high fire load of ro-ro decks and the effectiveness of existing sprinkler systems. Their report, draws two interesting conclusions:

1. The international shipping industry should coordinate their efforts and their knowledge in this area.
2. A program with large-scale fire tests should be carried out to increase our understanding regarding fires and fire scenarios on ro-ro decks. In such a program, factors such as the type of combustible materials, ignition sources, vehicle size, vehicle breakdown on the deck, the position of sprinklers, water discharge densities ventilation flow rates, fire detection, additives to the water, drainage, etc., should be studied.

Moreover, it was proposed that the ability to use “water mist” systems or other types of fire-fighting systems be studied. The report and its conclusion were presented in a submission to the IMO FP51 in February 2007 [9].

In addition to the research described above, the EU project New European Ferry (NEF), whose outcome was presented in 2005, conducted an analysis of existing fire detection and water spray systems on ro-ro decks. Within the NEF project, better solutions were investigated with the help of CFD simulations [10].

The analysis shows that a spill fire consisting of diesel combined with fire in a freight truck reaches a fire power of around 200 MW when the water spray system is not activated. A sprinkler designed under current requirements would only reduce the fire to between 40 to 60 MW, mainly because the vehicles prevent the water from reaching the seat of the fire. Higher water discharge densities do not seem to be more effective because of the shielding effect. An alternative system with low-mounted foam (AFFF) nozzles and water mist nozzles at the ceiling limited the spill fire such that that the total fire power was reduced to around 20 MW.

The results are very consistent with results from the DESSO project that ended in 2005. Within the framework of that project [11] the impact of a fire was examined and how an improved sprinkler systems could be designed. The calculations showed that a fire starting during loading or unloading is the most critical case, because the access of air (oxygen) is good. As a consequence of these findings, it was suggested that the deck space is divided into smaller volumes with fire-resistant textiles and that a “water mist” system is used to increase the cooling capability within this zone.

It should be added that there are fire test procedures and installation guidelines for “alternative” systems for ro-ro decks. These requirements were adopted by IMO in

1999 as an alternative option in MSC/Circ. 914 [12]. Presently there is, however, no system on the market that meets these requirements.

During 2005 and 2006, SP Fire Technology worked together with Marioff Corporation Oy, Det Norske Veritas and VTT Technical Research Centre of Finland to develop an alternative testing method to MSC/Circ. 914. The work is described in references [13] and [14]. A draft of the fire test procedure [15] was presented at IMO FP51 in February 2007. It is important to emphasize that the test method is adapted to the effectiveness of the system prescribed in Resolution A.123 (V), i.e., an alternative system would not be expected to exhibit better performance than Resolution A. 123 (V). The installation guidelines and fire test procedures were adopted by the Maritime Safety Committee in 2008 and published as MSC.1/Circ. 1272 [16] which supersedes MSC/Circ. 914.

However, it was clearly stated in the working group at IMO working with these issues that the long-term goal should be to replace the requirements of Resolution A.123 (V).

1.2 The scope of the project

Although major fires on ro-ro deck are relatively rare, according to a study conducted by Det Norske Veritas [17], they can have serious consequences. A recent example is the fire on board the ro-ro cargo ship Und Adriyatik in February 2008. The fire started in the main deck area (the reason is under investigation) and spread to several decks very rapidly. Fortunately, there was no loss of human life and no pollution to the sea, but the fire wrecked all the accommodation, forward and aft decks and all the cargo to the degree that the ship was declared a constructive total loss [18].

As discussed above, there is a broad international consensus that the sprinkler systems installed on vehicles spaces and ro-ro cargo decks under the present requirements are outdated. Much has happened since the requirements were introduced more than 40 years ago.

Despite the fact that several international projects have touched on the issue in recent years, none of the projects have had the objective to develop concrete recommendations for more efficient sprinkler designs. The aim of this project is to develop a technical basis replacing the design and installation guidelines of Resolution A.123 (V). The last stage of the project is to formulate recommendations and to present them for the working group within the IMO which is currently working on these issues.

The intention is that the project will contribute to increased fire safety while also reducing the risks associated with vessel stability by providing fire protection alternatives that reduces the volumes of water used during fire fighting activities.

The project started with an evaluation of fires and fire scenarios in reduced scale, see SP Report 2008:42 [19], and water distribution tests using both a traditional water spray system and a high-pressure water mist system [20].

1.3 The geometrical dimensions of freight trucks

The geometrical dimensions of freight truck vehicles in Europe are regulated in EU Directive 96/53/EC which amends the maximum authorised dimensions and also applies to vehicles used in national traffic. The maximum vehicle length is 18,75 m and the maximum width is 2,55 m (2,60 m for refrigerated vehicles). The restrictions on height (4,0 m) and weight (40 tonnes) authorised for international traffic are not extended to national traffic.

Sweden and Finland have an exception to the directive which allows freight trucks with trailers to be a maximum of 25,25 m long. In addition, it is common that the freight trucks are up to 4,50 m high. Typical freight truck and trailer combinations used in these countries are shown in figure 1.

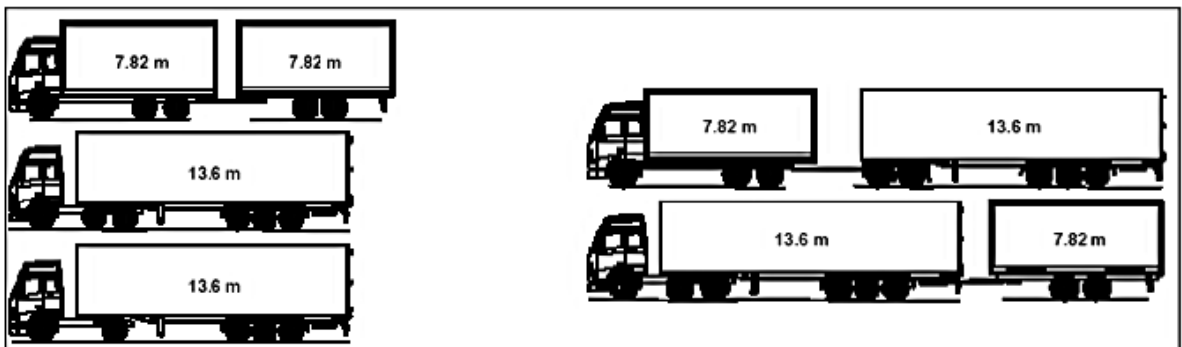


Figure 1 Typical freight truck and trailer combinations in Sweden and Finland [21].

Trailers covered by tarpaulins are common in Europe, refer to figure 2, but not as common in the Nordic countries, due to the climate. In these countries solid boxes are used. The walls and ceiling of these boxes are usually made from a sandwich panel with outer sides of 2 mm plastic sheets and a core made from either plywood, polyurethane (PU) or expanded polystyrene (EPS). The overall thickness is typically 20 mm. The parts are glued together and then put into a framework of aluminium profiles.

For the transportation of food or other products that require a lower than ambient temperature, the walls and ceiling of such a box are usually up to 45 – 55 mm thick with a core of EPS, refer to figure 3.

The dimensions and loading capacity of a trailer for the transport of dry, packed and non temperature-sensitive cargo is typically:

- Length: 13,60 m.
- Width (internal): 2,45 m - 2,50 m.
- Height (internal): 2,50 m - 3,00 m.
- Capacity: Up to 34 Euro pallet spaces.

Freight trucks for shorter distance transportations usually have a door at the rear, with a lift to load and unload the cargo. Freight trucks and trailers for long haulage transports have in addition, doors on one or both sides, for easier access to the cargo.



Figure 2 A common type freight truck used throughout Europe, where the trailer is covered by a tarpaulin, both on the sides (“curtain sides”) and over the top.



Figure 3 A common type freight truck used for temperature controlled (freezer or refrigeration) transportation of for example food products.

1.4 The scope of the tests described in this report

The IMPRO project was built on the experience that emerged from previous projects, primarily that of the references [3] and [13]. The results of these past projects show that the evaluation of sprinkler system efficiency need not be made in large-scale fire tests.

The fire tests were therefore conducted using a mock-up trailer with authentic geometry and designed to vary the following parameters:

- The system technology, i.e. a traditional water spray system or high-pressure water mist system.
- The water discharge density.
- The water pressure (water spray system only) maintaining the water discharge density, thereby varying the droplet size and the momentum of the water spray.
- The exposure of the fire, i.e. the use of a roof on the trailer mock-up.

Full details of the test set-up are given in the next chapter.

2 The fire test set-up

2.1 The trailer mock-up

The mock-up was constructed to geometrically replicate a typical trailer of a freight truck except that the overall length was shorter than in reality. Table 1 shows the dimensions of the trailer mock-up.

Table 1 The dimensions of the trailer mock-up.

Dimensions	Dimensions [m]
Length	5,50
Width	2,60
Overall height	4,00
Height of cargo space*	2,80
Height of cargo platform above ground	1,10

*) When the roof of the 'trailer' was in use.

The mock-up was constructed from 100 mm square iron and the bottom and the roof of the platform of the mock-up was constructed from nominally 4 mm thick steel plates. Tests were conducted both with and without a roof over the cargo space of the trailer model.

Six rows of commodity (see a detailed description below) were positioned on the platform such that longitudinal and transversal gaps of 100 mm were created between the stacks of commodity, see figure 4.

For the tests with the roof of the trailer mock-up the amount of commodities was reduced to two rows, i.e., one third of the amount of commodity used for the tests without the roof, see figure 5.



Figure 4 An illustration of the arrangement of the commodity on the trailer mock-up, showing the steel screen on the right hand long side. A similar screen was positioned on the left hand side.



Figure 5 The trailer mock-up with the roof installed. Note that less amount of commodity, two instead of six rows was used for these tests.

2.2 The target screens

A steel screen was positioned parallel with the long sides of the trailer mock-up. The screens had a height (2,80 m) that corresponded to the height of the ‘cargo space’ of the mock-up. The tops of the screens were levelled with the top level of the roof over the trailer mock-up, i.e., 4,00 m above floor level. The length of 2,70 m was shorter than the overall length of the mock-up, but covered the two central stacks of commodity and extended halfway along the length (on either side) of the adjacent stacks.

The surface temperatures of the steel screens were measured at eighteen (18) different measurement points, see the description under “Instrumentation and measurements”. The nominal thickness of the steel sheets used for the screens was 0,8 mm and the front face of the screens were painted black using heat-resistant paint.

2.3 The commodity

The EUR Std Plastic commodity consists of empty Polystyrene (PP) cups without lids, placed upside down (i.e. open end down), in compartmented cartons, 120 cups per carton. The cartons measures 600 mm × 400 mm × 500 mm (L × W × H) and are made from single-wall, corrugated cardboard. When compartmented, the cartons are divided into five layers using corrugated sheets, with each layer divided into 24 compartments by over-locking corrugated cardboard partitions, forming a total of 120 compartments where the plastic cups are placed [22]. Refer to figure 6.

When used on standard 1200 mm × 800 mm EUR pallets, eight cartons are placed on each pallet. The overall dimension of one pallet load is consequently 1200 mm × 800 mm × 1000 mm (L × W × H) plus the height of the pallet (nominally 150 mm).

The commodity contains 960 polystyrene cups per pallet load.

The individual cups have a measured average weight of 28,2 g, correlating to a total weight of the plastic of 3,4 kg per carton. The overall weight of one carton including the cups is approximately 5,4 kg. The total weight (excluding the pallet) of one 1200 mm × 800 mm pallet load of the commodity is approximately 43,2 kg of which approximately 63% by weight was plastic, excluding the pallet. If the weight of the wooden pallet is included in this estimation, approximately 42% by weight is plastic.

For the tests, cartons were placed on a standard EUR wood pallet and the individual cartons were stapled against the wood pallet to increase stability, see figure 6. Two pallets loads were positioned on top of each which equalled an overall height of approximately 2,3 m. The vertical distance measured from the top of the commodity to the underside of the roof of the trailer mock-up (when used) was 0,5 m.



Figure 6 One pallet load of the EUR Std plastic commodity (left) with a close-up photo of the arrangement of the plastic cups in the individual cartons (right).

When developed, the intention was to make the EUR Std Plastic commodity as similar as possible to the FM Global Std Group A Plastic commodity, i.e. using the same type materials, approximately the same overall size, the same number of cups, the same density of plastic, etc. However, the commodity had to fit the pallet size dimensions used within Europe. Because of the different geometry of the cartons, as compared to the ‘original’ commodity, the plastic cups had to be made slightly smaller and lighter, although the cup was designed for approximately the same wall and bottom thickness as the FM Global cup. The amount of plastic per pallet load of commodity is, however, identical.

The FM Global Standard Plastic Commodity and the FM Global Class II Commodity⁴ have been widely used in the fire protection community as two representative “benchmark” warehouse fire hazards for evaluation of sprinkler fire protection performance in large-scale fire tests since the 1970’s.

Although the EUR Std Plastic commodity does not represent the most severe commodity that can be found on a freight truck trailer in practice, it was considered representative of a high hazard commodity. The fact that it is established as a “benchmark” commodity in large-scale sprinkler fire tests made it logical to use in these tests.

⁴ The FM Global Class II Commodity consists of double triwall cartons with a steel liner inside. Non-combustible products in slatted wooden crates are defined as Class II commodities by NFPA 13. In this case, the packaging is contributing to the combustibility of the commodity. By contrast, the packaging may limit the involvement of the material inside. Exposed plastic commodities, for example, require higher sprinkler densities than the same plastic contained in corrugated cartons since the cartons absorb sprinkler water and delay involvement of the plastic material.

2.4 The potential severity of the fire load

Due to the high fire load, free-burn fire tests were not feasible. However, based on down-scaled (scale 1:4) fire tests conducted prior to the test programme [19] an estimation of the severity of the fire load under free-burn conditions is possible.

Figure 7 shows the calculated total heat release rate for a test set-up consisting of six and two rows of commodity, respectively. For the later case, a solid roof over the set-up was used.

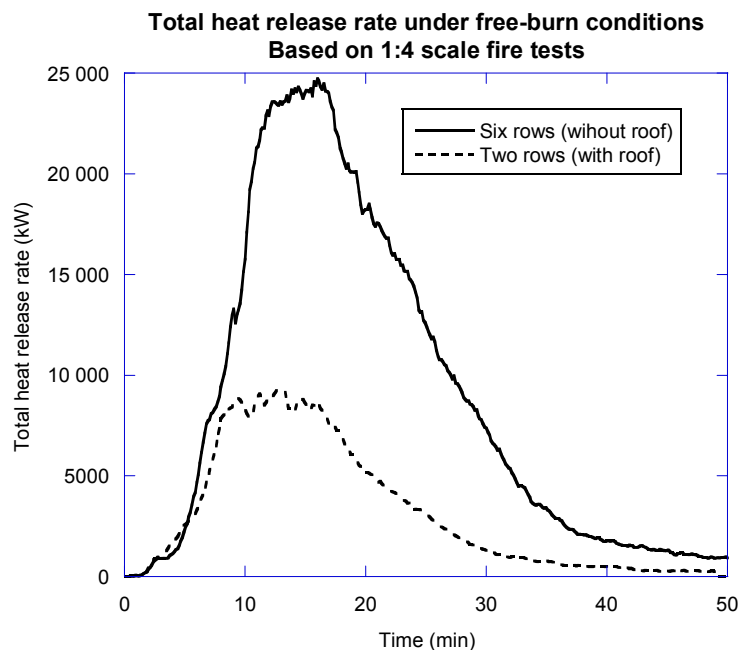


Figure 7 The potential severity of the test set-up based on down-scaled fire tests.

The tests indicates that six rows of commodity has the potential for a peak total heat release rate of almost 25 MW and two rows has the potential for a peak total heat release rate around 9 MW.

2.5 Air velocities around the test set-up

The ventilation system of the fire test hall and the ventilation flow of the Industry Calorimeter (see the description below) generate an air flow inside the fire test hall. During these tests, the ventilation flow rate of the fire test hall was 100 000 m³/hour and the ventilation flow rate of the Industrial Calorimeter 110 000 m³/hour, i.e. the total ventilation flow rate of the fire test hall was 210 000 m³/hour or 3500 m³/min.

The air velocities around the test set-up were determined prior to a couple of tests and the results were as follows, refer to table 2.

Table 2 The measured air velocities around the test set-up.

Position	Velocity in vertical direction [m/s]	Velocity in horizontal direction [m/s]
At floor level	0,10	0,53
At bottom level of the trailer platform	0,10	0,02
At mid-height of the commodity (outside)	0,10	0,11
At top of the commodity stacks (outside)	0,25	0,16
At the point of fire ignition	0	0,07
Inside the central stacks of commodity, at mid-height	0,29	0,08
Inside the central stacks of commodity, at the top	0,34	0,07

3 The fire suppression systems

3.1 The system pipe-work

The piping arrangement for the water spray system was fabricated consisting of a double feed tree system. The system consisted of four DN50 (2") branch lines with nozzle connections for eight nozzles at a 3,2 m × 3,0 m nozzle spacing, i.e. a coverage area of 9,6 m² per nozzle. The system was fed through a DN65 (1½") main that was connected to the public main via a pump. The pipe-work and the position of the nozzles relative to the trailer mock-up is shown in figure 8.

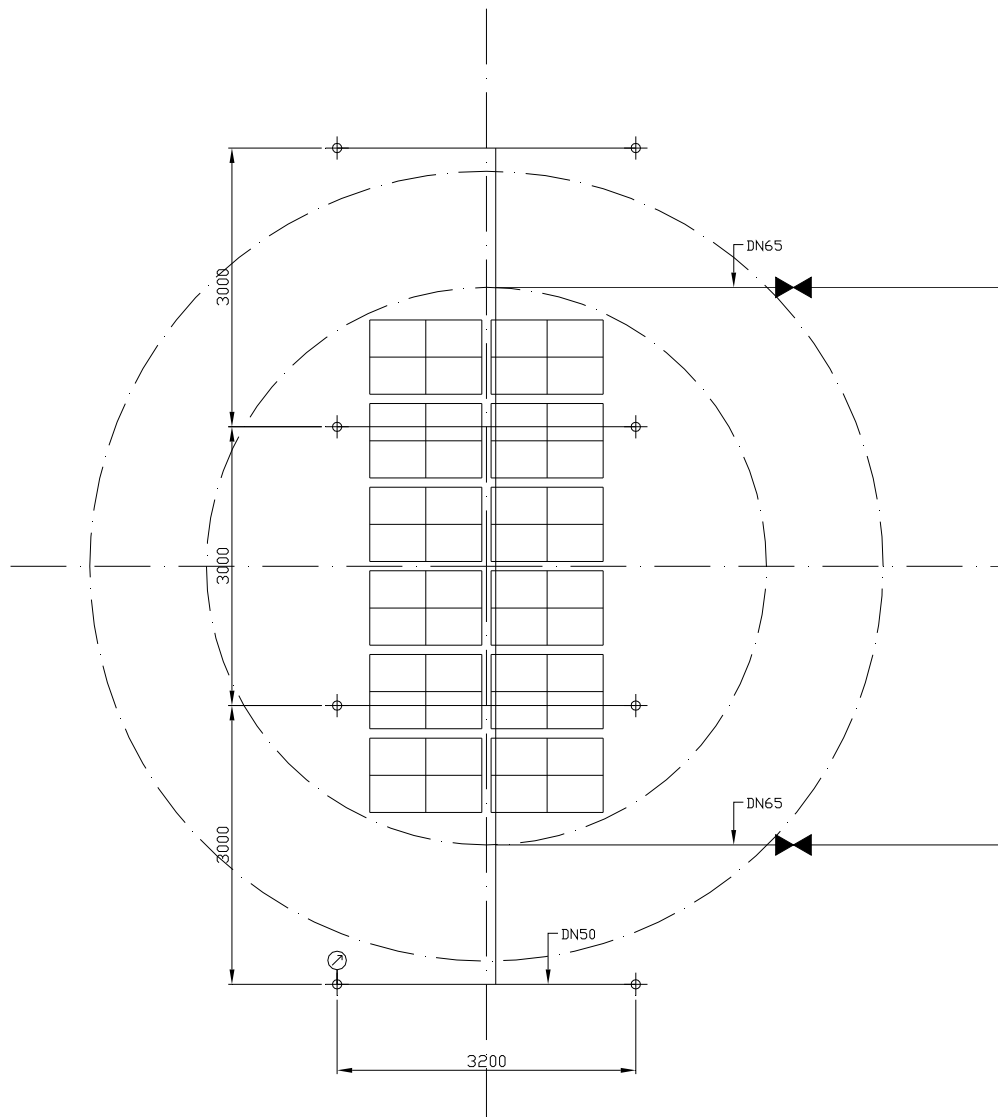


Figure 8 The pipe-work and the position of the nozzles relative to the trailer mock-up in the top view.

The piping arrangement for the high-pressure water mist system was constructed in a similar fashion, except that DN12 branch lines were used and the system was fed from one connection point only. The piping for the high-pressure water mist system was attached directly below the piping for the water spray system, which was elevated to keep the vertical distance from the tips of the water mist nozzles to the top of the test set-up analogous. The water spray system was therefore fully functional and used as a safety precaution during the water mist tests.

The position of the nozzles relative to the trailer mock-up from the short side view is shown in figure 9. The vertical distance measured from the nozzles to the roof (when used) of the trailer mock-up was 0,5 m and the vertical distance to the top of the stacks of commodity approximately 1,0 m.

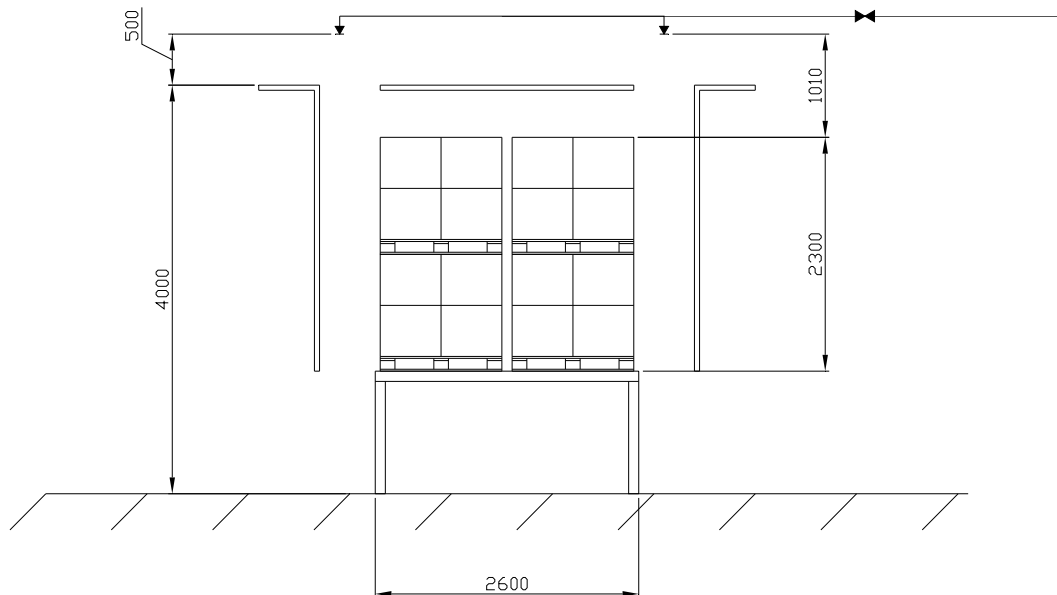


Figure 9 The position of the nozzles relative to the trailer mock-up from the short side view.

3.2 The medium velocity nozzles

The medium velocity nozzles used for the water spray system were open (non-automatic), pendent directional discharge water spray nozzles. The nozzles had an external deflector that discharged a uniformly filled cone of medium velocity water droplets. The nozzles used in the tests had no nozzle strainer.

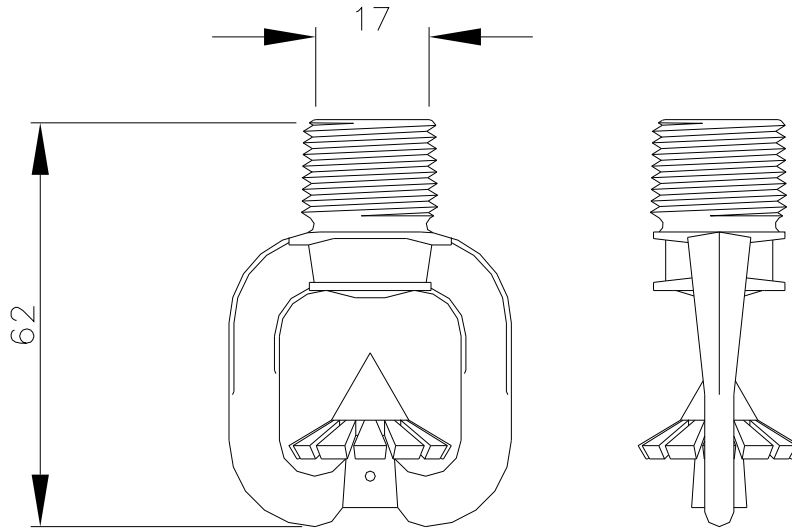


Figure 10 A principle drawing of the open (non-automatic) medium velocity nozzles used with the water spray system. The actual nozzles used in the test have a horizontal deflector.

The nozzles are available in a wide variety of orifice sizes and spray angles, however, the types listed in table 3 were used during these tests.

Table 3 The medium velocity nozzles used in the tests.

Nozzle designation	K-factor [metric]	Minimum orifice diameter [mm]	Spray angle [°]
Protectospray D3, No. 24	43,2	8,33	180
Protectospray D3, No. 28	59,0	9,53	180
Protectospray D3, No. 32	80,6	11,13	180
Protectospray D3, No. 34	103,7	12,70	180

The recommended discharge pressures range from 1,4 bar to 4,1 bar. Discharge pressures in excess of 4,1 bar will result in a decrease in coverage area since the spray pattern tends to draw inwards at higher pressures. The maximum recommended working pressure is 12,1 bar.

The nozzle pressures ranged from 1,2 to 4,9 bar during the tests.

The nozzles were installed with their frame arms parallel with the longitudinal flue between the trailer mock-up and the steel screens on either sides.

The nozzles were provided by TYCO Fire Suppression & Building Products.

3.3 The high-pressure water mist nozzles

These nozzles were open (non-automatic) multi-orifice nozzles without any external deflector. When spraying, the nozzle discharge forms a solid cone-shaped spray pattern of high velocity jets that breaks up into small water droplets a relatively short distance from the nozzle orifices. The overall spray angle is approximately 160° .

The K-factor of the nozzles was 3,6, 4,4 and 6,1 (metric), respectively. The recommended discharge pressures range from 60 bar to 120 bar. The tests were conducted at either 100 bar or 84 bar.

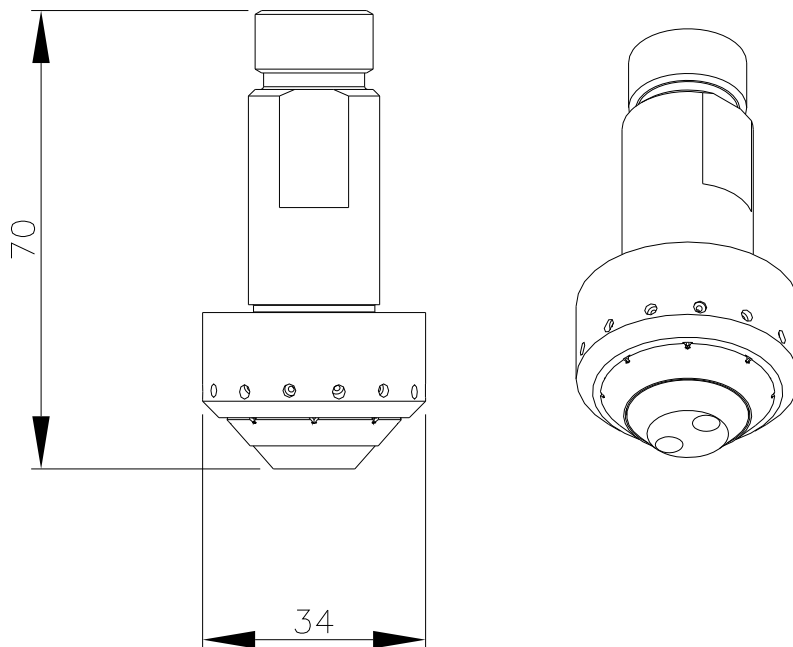


Figure 11 A principle drawing of the open (non-automatic) high-pressure water mist nozzles used in the tests.

The nozzles and the associated equipment were provided by Ultra Fog AB.

4 Instrumentation and measurements

4.1 The Industrial Calorimeter

The tests were conducted under the Industrial Calorimeter, a large hood connected to an evacuation system capable of collecting all the combustion gases produced by the fire. The hood is 6 m in diameter with its lower rim 7,2 m above the floor. For these tests, a cylindrical fibreglass "skirt", hanging from the lower rim of the hood, was used to increase the gas collecting capacity of the hood. In the duct connecting the hood to the evacuation system, measurements of gas temperature, velocity and the generation of gaseous species such as CO₂ and CO and depletion of O₂, can be made.

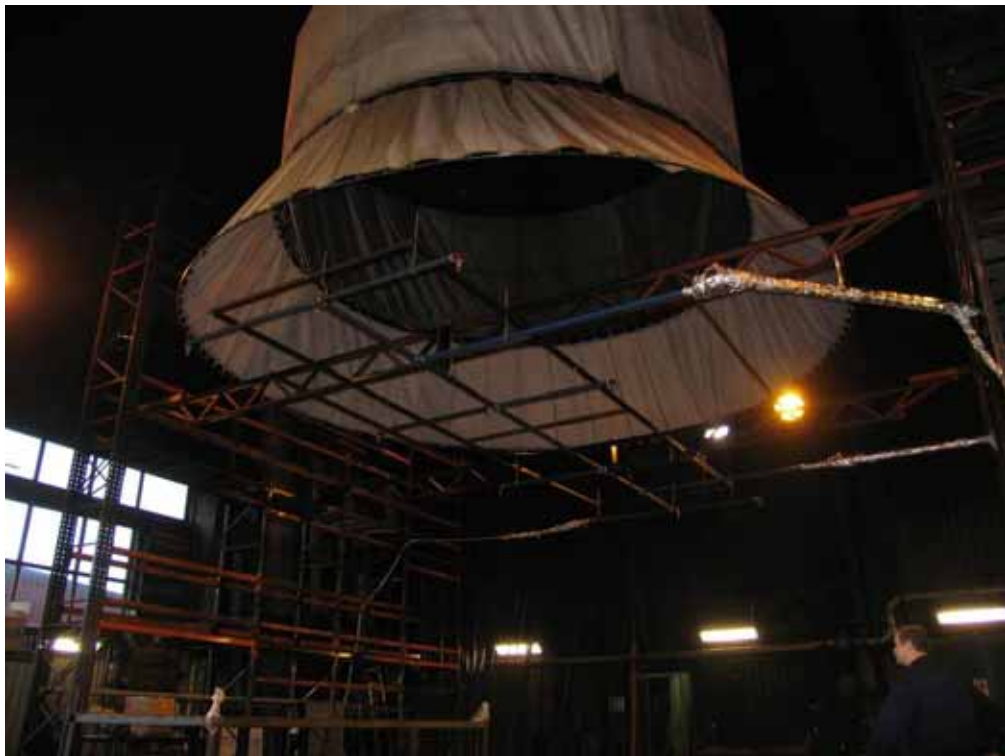


Figure 12 The Industrial Calorimeter was used to measure the heat release rates from the fires. The pipe-work for the water spray system can be seen in the photo.

Based on these measurements, both the convective and the total heat release rate can be calculated. These, and the other parameters described below, were used for the evaluation of the test results.

HRR_{conv}: The convective heat release rate measured during a test is calculated on the basis of the gas temperature and mass flow rate in the calorimeter system. The convective fraction of the total heat release varies with the fuel and other factors, but usually approximately two-thirds of the energy generated by a fire is released through convection. Additionally, the convection produces the velocities and temperatures in the fire plume. The velocity and temperature in the fire plume determines the rate of heat transfer, i.e., the convective heat release rate is also

responsible for the activation of sprinklers and the heating of the overhead ceiling or deck. The maximum convective heat release rate is, therefore, one of the most important quantities for characterising fire severity.

For these tests, the maximum “one minute average” was calculated. This figure is preferred over the instantaneous maximum as spikes due to, e.g., environmental changes, electrical noise, etc, have minimal influence on the value.

HRR_{tot}: The total heat release rate measured during a test is calculated on the basis of the oxygen depletion of the fire, as measured in the calorimeter system. HRR_{tot} is comprised of both the convective and radiative heat release rate, as well as the heat being conducted away and absorbed within the test set-up. During the fully developed stage of a fire, however, heat conduction and absorption is relatively small compared to the convective and radiative components. Radiation is the primary mechanism by which fire spreads across aisles and other open spaces to adjoining combustibles. It is also, in part, responsible for lateral fire spread throughout a large fuel array, as well as an overall fundamental measure of fire severity.

This parameter was also calculated as the maximum “one minute average”.

The total convective energy: The energy convected upwards is largely responsible for the heating of the exposed steel at the ceiling (or a steel deck) and the activation of automatic sprinklers. The total convective energy, calculated from fire ignition until the termination of a test does help to characterise fire severity, as in the case of heat transfer duration is as important as magnitude. Some fires are very intense but short-lived and their thermal impact may be less severe than a fire of lower intensity with a longer duration. The total convective energy is an important measure of a fire's maximum potential for causing thermal damage.

The total energy: The total energy, in this case determined from fire ignition until the termination of a test, is a measure of the amount of combustibles being consumed.

4.2 Surface temperature measurements

The surface temperatures of the steel plates positioned along both long sides of the trailer mock-up were measured at eighteen (18) different measurement points, on each of the steel plates. Three of the measurement points were positioned on the horizontal top surface of the steel plate and the remaining fifteen measurement points on the vertical surface facing the trailer mock-up.

The measurements were made with (Type K) thermocouples having a diameter of 0,5 mm that were welded directly to the back side of the steel plate. All the temperature measurement points and the associated channels are shown in table 4.

Table 4 The temperature measurement points and the associated channels

Measurement channels		Position
Right hand side screen	Left hand side screen	
C21	C41	Horizontal top surface
C22	C42	Horizontal top surface (midline)
C23	C43	Horizontal top surface
C24	C44	Vertical surface, 250 mm below top
C25	C45	Vertical surface, 250 mm below top (midline)
C26	C46	Vertical surface, 250 mm below top
C27	C47	Vertical surface, 750 mm below top
C28	C48	Vertical surface, 750 mm below top (midline)
C29	C49	Vertical surface, 750 mm below top
C30	C50	Vertical surface, 1250 mm below top
C31	C51	Vertical surface, 1250 mm below top (midline)
C32	C52	Vertical surface, 1250 mm below top
C33	C53	Vertical surface, 1750 mm below top
C34	C54	Vertical surface, 1750 mm below top (midline)
C35	C55	Vertical surface, 1750 mm below top
C36	C56	Vertical surface, 2250 mm below top
C37	C57	Vertical surface, 2250 mm below top (midline)
C38	C58	Vertical surface, 2250 mm below top

4.3 System water pressure and water flow rate measurements

The system water pressure (C78) was measured at the pump unit and at the pipe-work grid, using Transinstrument 2000A pressure transducers. The total water flow rate (C39) was measured using a Krohne 0 – 2000 L/min flow meter.

The total water flow rate of the high-pressure water mist system was not measured. It was calculated based on the measured system pressure and the K-factor of the nozzles.

5 The fire test series and fire test procedures

5.1 The fire test series

The following fourteen fire tests were conducted with and without the roof of the trailer mock-up, refer to tables 5 and 6, respectively.

Table 5 Fire tests conducted without the roof of the trailer mock-up.

Test no.	System	Nominal discharge density [mm/min]	System operating pressure [bar]	Water flow rate per nozzle [L/min]	Total water flow rate [L/min]
1E(15)	Water spray	15	1,9	144	1152
2E(10)	Water spray	10	1,4	96	768
3E(10)	Water spray	10	4,9	96	768
4E(5)	Water spray	5	1,2	48	384
5E(HP-3,75)	Water mist	3,75	100	36	288
6E(HP-4,6)	Water mist	4,6	100	45	360
7E(HP-5,8)	Water mist	5,8	84	56	447
8E(10)*	Water spray	10	4,9	96	768

*) Manually activated at a convective heat release rate of 6 MW instead of 3 MW.

For the tests with the roof of the trailer mock-up, the amount of commodity was reduced to two rows, i.e., one third of the amount of commodity used for the tests without the roof.

Table 6 Fire tests conducted with the roof of the trailer mock-up.

Test no.	System	Nominal discharge density [mm/min]	System operating pressure [bar]	Water flow rate per nozzle [L/min]	Total water flow rate [L/min]
1S(15)	Water spray	15	1,9	144	1152
2S(10)	Water spray	10	1,4	96	768
3S(10)	Water spray	10	4,9	96	768
4S(5)	Water spray	5	1,2	48	384
5S(15)*	Water spray	15	1,9	144	1152
6S(HP-5,8)	Water mist	5,8	84	56	447

*) Repeat of Test 1S(15) due to a leakage of the roof.

As indicated, some of the fire tests were repeated with a nozzle and pressure combination creating smaller droplets, as one of the intentions of the tests was to investigate the influence of the water droplet size on the performance of the system. Therefore, parallel tests were conducted at a discharge density of 10 mm/min both with and without the roof of the trailer mock-up.

When the discharge density of the high-pressure system was increased to 5,8 mm/min, the capacity of the pump unit was exceeded and the system operating pressure decreased to 84 bar.

The nozzles used in the tests, their K-factor, nominal water discharge density, system operating pressure and estimated media droplet size are summarised in table 7.

Table 7 The nozzles that were used and the corresponding nominal water discharge density, K-factor, system operating pressure, orifice size and estimated median droplet size.

Nominal discharge density [mm/min]	Nozzle K-factor	System operating pressure [bar]	Minimum orifice diameter [mm]	Nozzle designation	Estimated median droplet size [µm]
Medium velocity nozzles					
5	43,2	1,2	8,3	D3, No. 24	889
10	80,6	1,4	11,1	D3, No. 32	1028
10	43,2	4,9	8,3	D3, No. 24	559
15	103,7	1,9	12,7	D3, No. 34	1014
Water mist nozzles					
3,75	3,6	100	--	Ultra Fog HP	~150
4,6	4,4	100	--	Ultra Fog HP	~150
5,8	6,1	84	--	Ultra Fog HP	~150

Note: 1 bar = 100 kPa.

The median water droplet size for the medium velocity nozzles was estimated using a correlation for the median droplet size with operating pressure and orifice size developed by Heskestad [23], i.e.:

$$d_m = 1.076 \Delta P^{-1/3} D^{2/3}$$

Where d_m is the volume median diameter in mm for the entire spray,
 ΔP is the operating pressure in kPa,
 D is the orifice diameter in mm.

This correlation has been found to be valid for geometrically similar nozzles, as would be the case for the medium velocity nozzles used in the tests.

The water droplet size of the water mist nozzles was estimated by Ultra Fog AB based on droplet size measurements of a similar type nozzles.

5.2 The fire ignition source

The commodity was ignited at the flue, near the bottom of the central stacks using four standardised ignition sources positioned directly against the corrugated cartons. The ignition source consists of a cube, 60 mm × 60 mm × 75 mm, made from pieces of insulating fibre board. Each cube was soaked with 120 mL of heptane and wrapped in a polyethylene plastic foil bag prior to the test.



Figure 13 The standardised igniters that consisted of a cube from pieces of insulating fibre board soaked with heptane and wrapped in a polyethylene plastic foil bag.

5.3 Fire test procedures

The system was manually activated at a convective heat release rate of 3 MW, which equalled a total heat release rate of approximately 5 MW. Photos of the fire size at the manual activation of the system are shown in the figures below.

For Test 8(10), the system was manually activated at a convective heat release rate of 6 MW, which equalled a total heat release rate of approximately 10 MW. The intent of the test was to explore the fire suppression capabilities against a fire twice as large as in the other tests.



Figure 14 The fire size at the manual activation of the system for the tests without the roof of the trailer mock-up, here exemplified with Test 4E(5). Time 01:58 [min:sec] after fire ignition.



Figure 15 The fire size at the manual activation of the system during Test 8E(10), where the fire size was twice as large as in the other tests. Time 02:33 [min:sec] after fire ignition.



Figure 16 The fire size at the manual activation of the system for the tests without the roof of the trailer mock-up, here exemplified with Test 5S(15). Time 02:13 [min:sec] after fire ignition.

6 Fire test results

6.1 Key parameters

Given below are tables summarizing the test results using the following heat release rate parameters:

- The peak total heat release rate (HRR_{tot}).
- The maximum one minute average total heat release rate.
- The peak convective heat release rate (HRR_{conv}).
- The maximum one minute average convective heat release rate.
- The total energy from 00:00 to 30:00 [min:sec], except where noted.
- The total convective energy from 00:00 to 30:00 [min:sec], except where noted.
- The ratio convective energy to total energy.

Heat release rate measurement graphs are given in section 6.2 and temperature measurement graphs in section 6.3.

Table 8 Test results for the fire the tests without the roof of the trailer mock-up, based on the heat release rate measurements.

Test	Peak HRR _{tot} [kW]	Max. one minute average HRR _{tot} [kW]	Peak HRR _{conv} [kW]	Max. one minute average HRR _{conv} [kW]	Total energy [MJ]	Convective energy [MJ]	Ratio convective to total energy
1E(15)	5292	4037	3225	2376	719*	219*	0,30
2E(10)	5705	5255	3614	3156	2329	686	0,29
3E(10)	5833	5079	3507	2887	1691	218	0,13
4E(5)	9636	9100	5306	5085	5149	2338	0,45
5E(HP-3,75)	18 813	N/A**	7698	N/A**	N/A**	N/A**	N/A**
6E(HP-4,6)	15 492	N/A**	6497	N/A**	N/A***	N/A***	N/A**
7E(HP-5,8)	14 848	14 397	7891	6737	11 065	4180	0,37
8E(10)	10 318	9356	6477	5270	2860	683	0,24

*) Measured from fire ignition to 10:00 [min:sec]. A very small fire was manually extinguished at 10:00 [min:sec].

**) Data not available. The fire was manually extinguished at 05:00 [min:sec] as the fire developed out of control of the system.

***) Data not available. The fire was manually extinguished at 05:30 [min:sec] as the fire developed out of control of the system.

Table 9 Test results for the fire the tests with the roof of the trailer mock-up, based on the heat release rate measurements.

Test	Peak HRR _{tot} [kW]	Max. one minute average HRR _{tot} [kW]	Peak HRR _{conv} [kW]	Max. one minute average HRR _{conv} [kW]	Total energy [MJ]	Convective energy [MJ]	Ratio convective to total energy
1S(15)	6056	5448	3837	3030	1941*	458*	0,23
2S(10)	6823	6571	3707	3457	4315	1785	0,41
3S(10)	6633	6224	3334	2761	4424	1332	0,30
4S(5)	8278	7962	4936	4566	5633	2789	0,50
5S(15)	7640	7465	3825	3649	4891	1657	0,34
6S(HP-5,8)	7117	6708	3092	2387	3516**	836**	0,23

*) Measured from fire ignition to 25:00 [min:sec] when the test was terminated. The roof over the trailer mock-up was leaking water and the test was repeated in Test 5S(15).

**) Measured from fire ignition to 14:00 [min:sec] when the test was terminated due to an unintentional pump stop.

Due to a short-circuit in the electrical power supply to the high-pressure pump unit, the application of water was stopped at 14:00 [min:sec] in Test 6S(HP-5,8).

A straightforward comparison of the total and convective energy over the full test duration time is, therefore, not possible. Table 10 shows a calculation of the total and convective energy over this shorter period of time, which allows a direct comparison of the performance of the systems.

Table 10 The total and convective energy as calculated from fire ignition to 14:00 [min:sec].

Test	Total energy [MJ]	Convective energy [MJ]	Ratio convective to total energy
1S(15)	1684	538	0,32
2S(10)	3157	1459	0,46
3S(10)	2988	1065	0,36
4S(5)	3944	2060	0,52
5S(15)	3588	1448	0,40
6S(HP-5,8)	3516	836	0,23

6.2 Heat release rate graphs

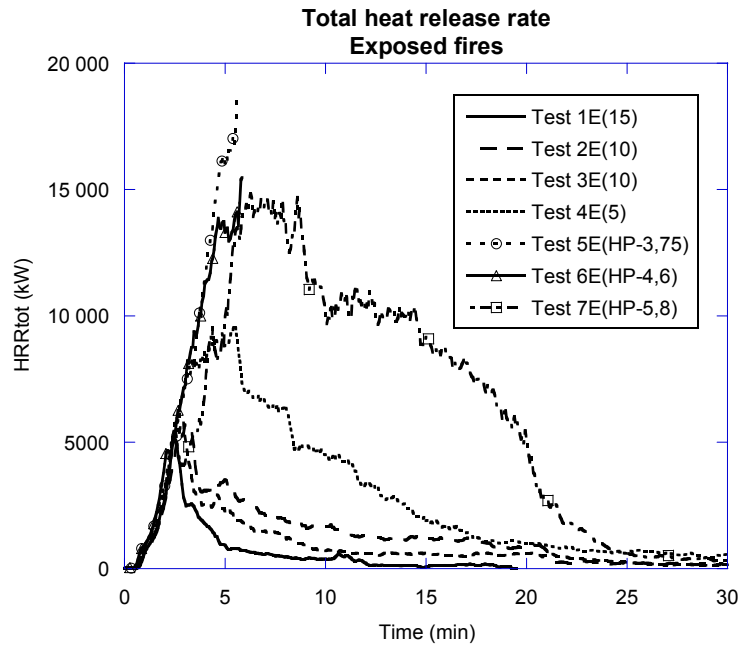


Figure 17 Total heat release rate histories for the fire tests without the roof of the trailer mock-up.

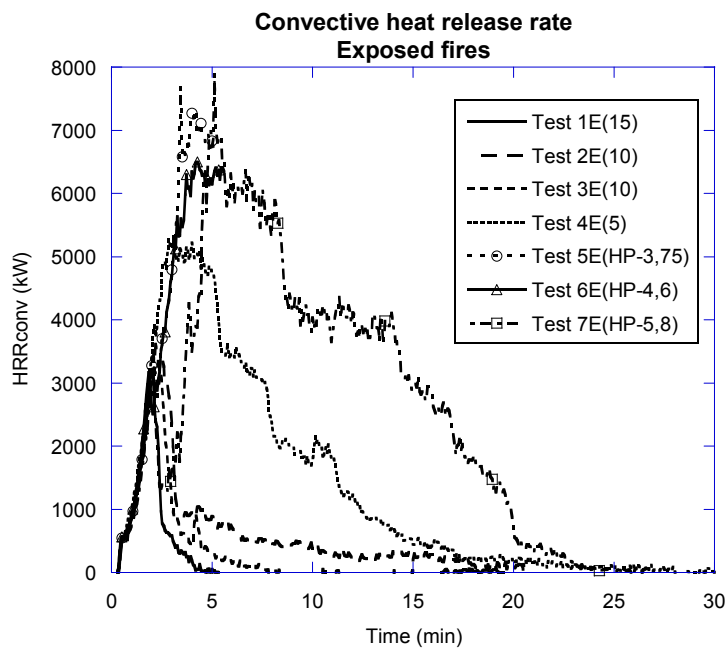


Figure 18 Convective heat release rate histories for the fire tests without the roof of the trailer mock-up.

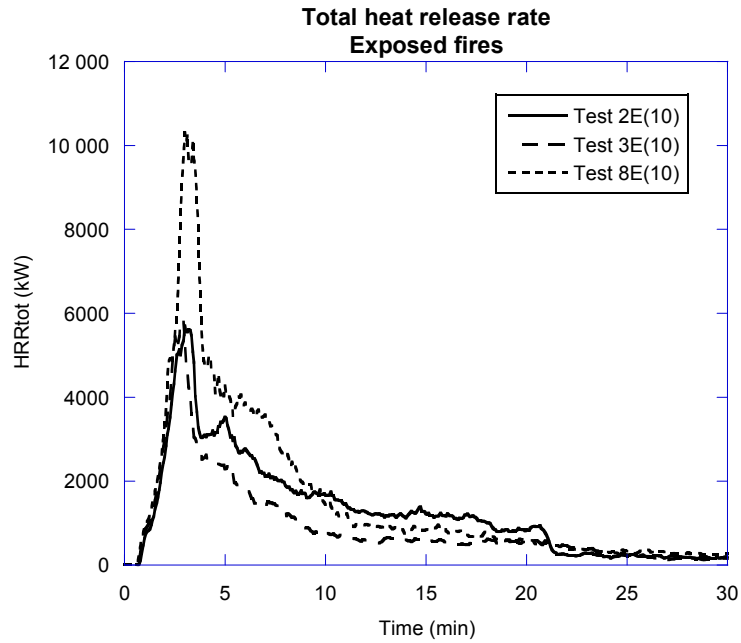


Figure 19 A comparison of the total heat release rate histories for the fire tests at 10 mm/min, including Test 8E(10). All tests without the roof of the trailer mock-up.

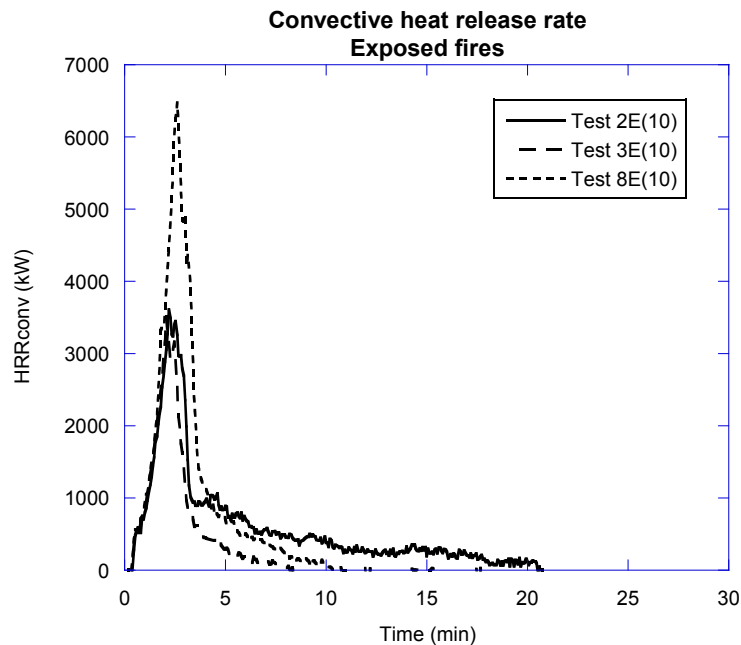


Figure 20 A comparison of the convective heat release rate histories for the fire tests at 10 mm/min, including Test 8E(10). All tests without the roof of the trailer mock-up.

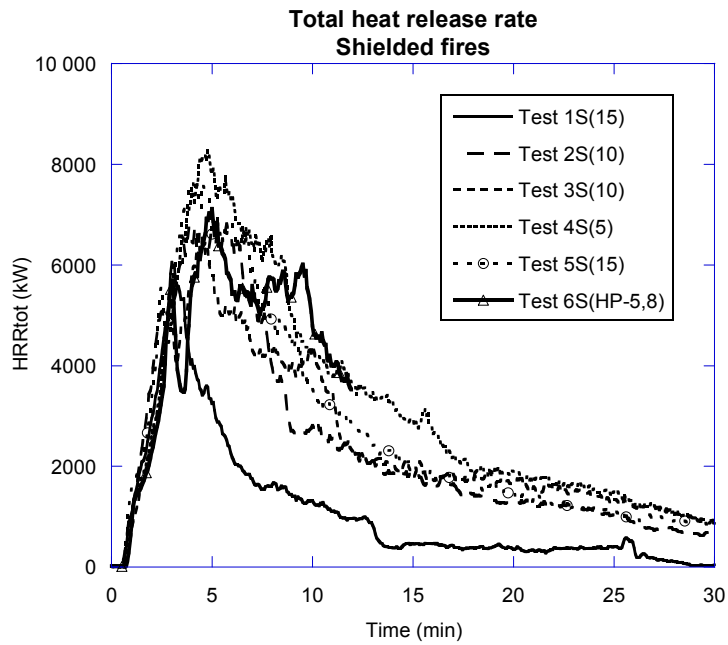


Figure 21 Total heat release rate histories for the fire tests with the roof of the trailer mock-up. Note: Leakage of the roof over the trailer in Test 1S(15).

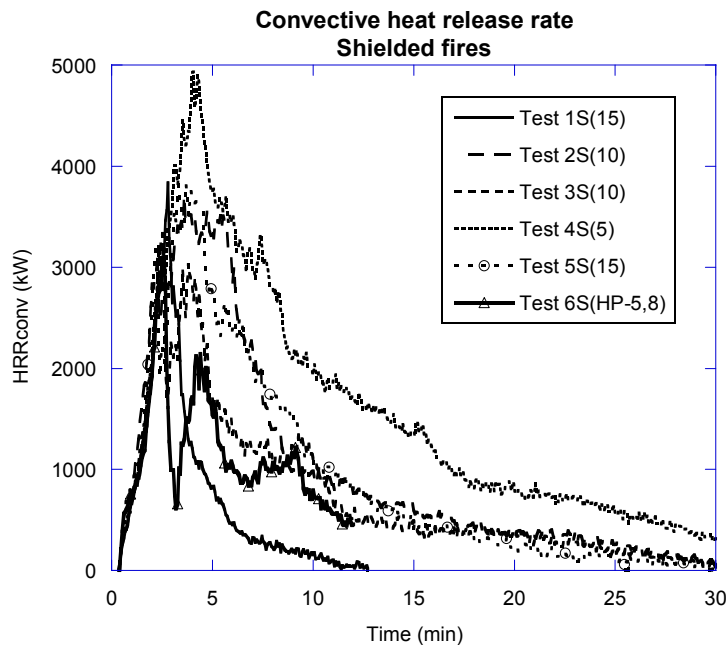


Figure 22 Convective heat release rate histories for the fire tests with the roof of the trailer mock-up. Note: Leakage of the roof over the trailer in Test 1S(15).

6.3 Temperature measurement graphs

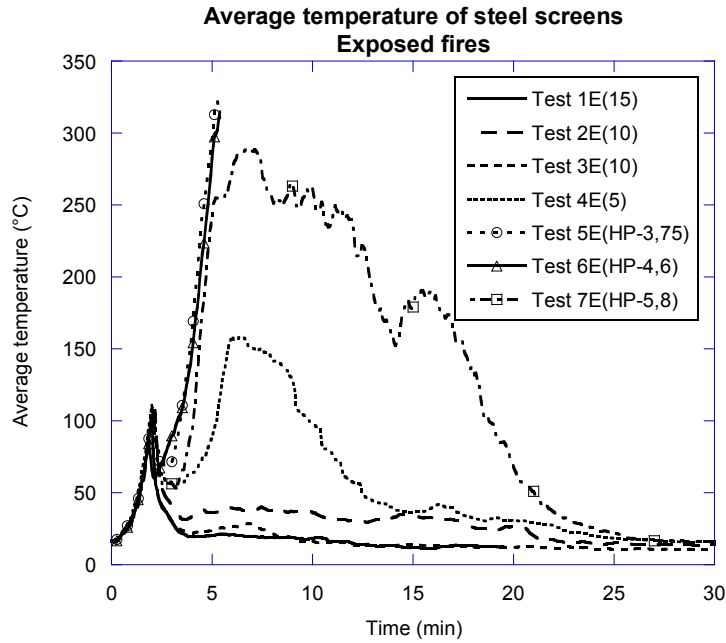


Figure 23 The average temperature of the steel screens for the fire tests without the roof of the trailer mock-up.

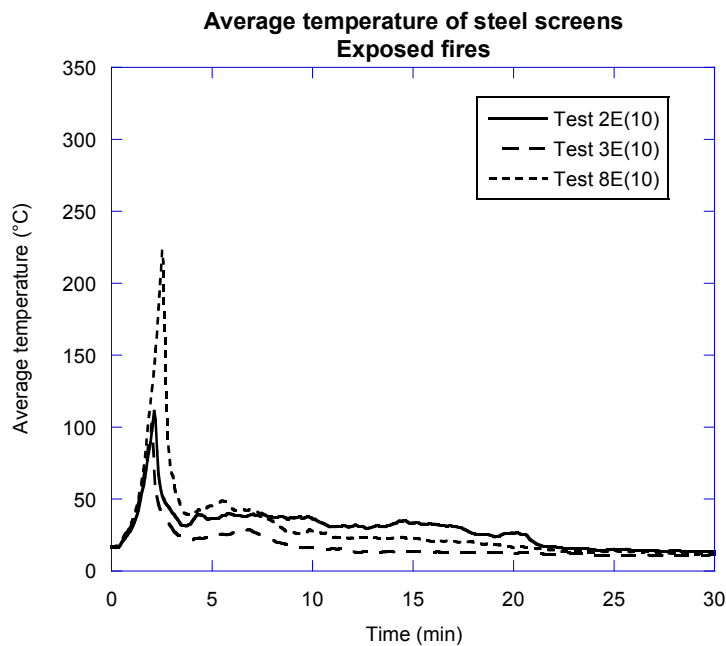


Figure 24 A comparison of the average temperature of the steel screens for the fire tests at 10 mm/min, including Test 8E(10). All tests were conducted without the roof of the trailer mock-up.

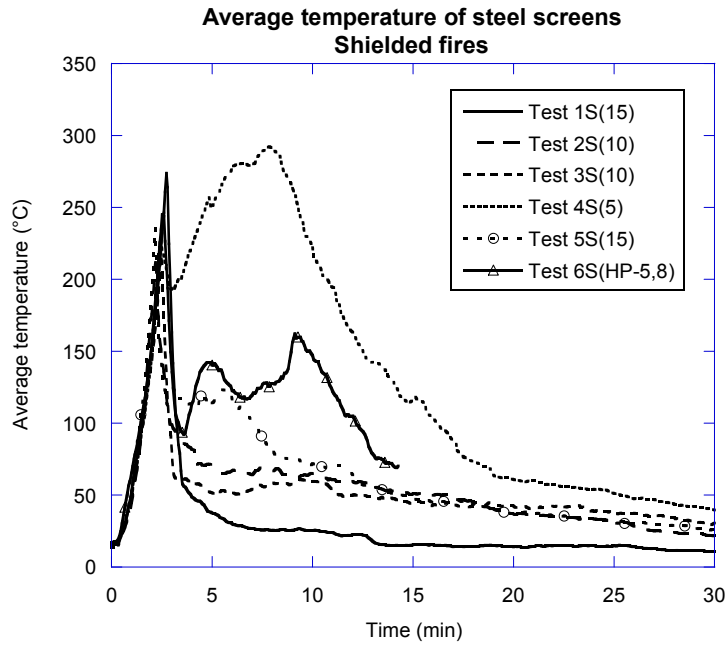


Figure 25 The average temperature of the steel screens for the fire tests without the roof of the trailer mock-up. Note: Leakage of the roof over the trailer in Test 1S(15).

7 Discussion

7.1 Fire tests without the roof of the trailer mock-up

Water spray system

The tests where the fires were fully exposed to the water spray show that there is a clear relationship between the level of performance and the water application rate. A discharge density of 15 mm/min provided immediate fire suppression, 10 mm/min fire suppression, and 5 mm/min fire control.

When discharging 10 mm/min at the higher system operating pressure, improved performance based on a comparison of both the total and convective energy, was achieved. This is an indication that smaller droplets improve system performance. The average temperature of the steel plates was also reduced, which would indicate that the risk for fire spread to adjacent vehicles is less. The maximum one minute average total and convective heat release rates were, however, similar to the test when 10 mm/min was discharged at a lower system operating pressure. This shows that the initial fire suppression capabilities were similar, irrespective of the system operating pressure.

For the final test, Test 8R(10), the activation of the system (10 mm/min at the higher system operating pressure) was intentionally delayed until the fire size was twice as large as in the other tests. Despite this, the fire was almost immediately suppressed.

High-pressure water mist system

The two first tests with the high-pressure water mist system were conducted at discharge densities of 3,75 and 4,6 mm/min, respectively. Both tests had to be terminated as the fires grew out of control of the system capabilities. To stop the fire growth, the water spray system, whose piping and nozzles had remained installed over the pipe-work of the mist system as a safety precaution, had to be manually activated. In both cases, the activation of the water spray system suppressed the fire immediately and the remaining fire was manually extinguished very easily. As the water flow meter of the water spray system was connected to the measurement system, it is possible to determine the water discharge densities that were applied when additional water was used. For Test 5E(HP-3,75), the application of water spray was started when the fire exceeded a total heat release rate of 18 MW and the water discharge density equalled almost 14 mm/min. For Test 6E(HP-4,6), the application of water spray was started when the fire exceeded a total heat release rate of 15 MW and the water discharge density was 14 mm/min.

The third fire test with the high-pressure water mist system, Test 7E(HP-5,8) was conducted with a water discharge density of 5,8 mm/min, which provided fire control. However, the maximum one minute average total and convective heat release rates were approximately twice as high for the test with the water mist system as compared to the water spray system at 5 mm/min. Visually it could also be

determined that considerably more combustible material was consumed during the water mist test.

The total and convective energy was also approximately twice as high for the test with the water mist system compared to the water spray system at 5 mm/min.

Figures 26 and 27 shows histograms of the maximum one minute average total and convective heat release rates and the total and convective energy, over the full test duration time, respectively, for all tests without the roof of the trailer mock-up.

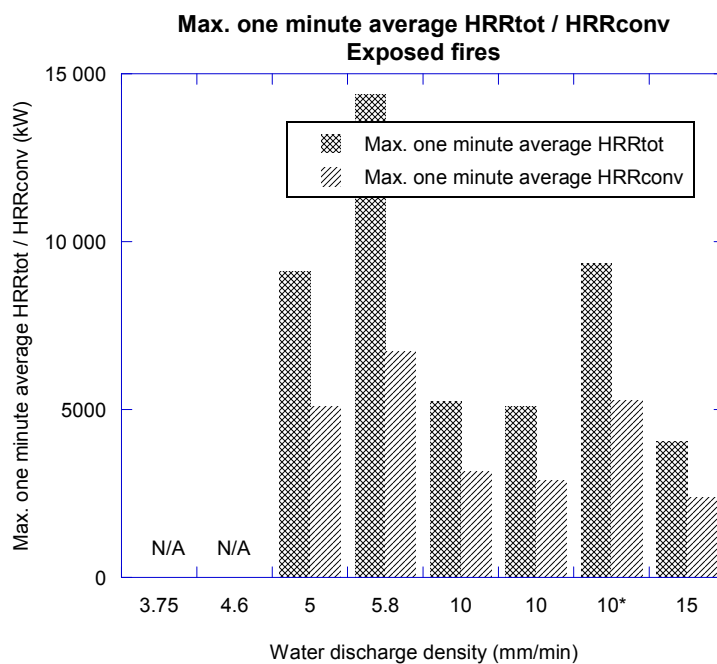


Figure 26 The maximum one minute average total and convective heat release rate for the fire tests without the roof of the trailer mock-up. The (*) indicates the test with delayed activation of the system.

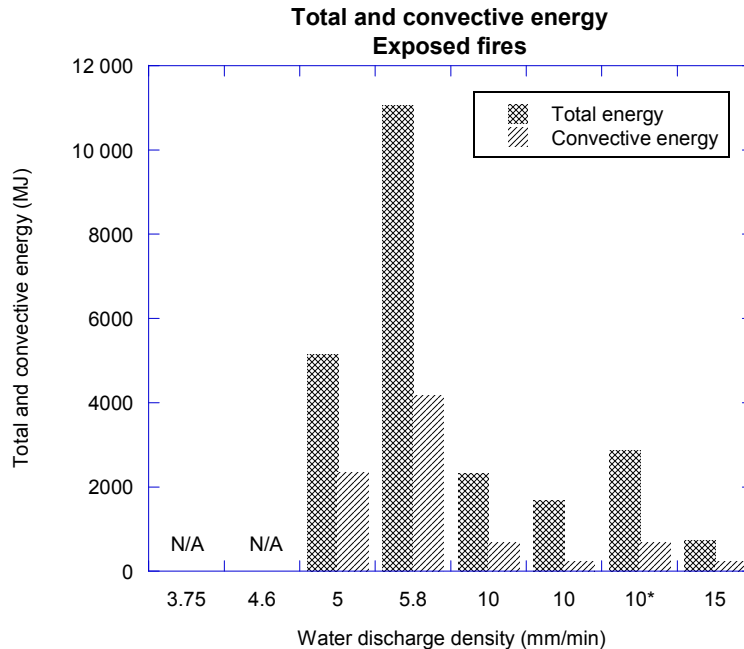


Figure 27 The maximum total and convective energy for the fire tests without the roof of the trailer mock-up. The (*) indicates the test with delayed activation of the system.

The average temperature of the steel plates on either sides of the trailer mock-up was significantly higher for the high-pressure water mist system at a water discharge density of 5,8 mm/min than the water spray system when discharging at 5 mm/min.

7.2 Fire tests with the roof of the trailer mock-up

Water spray system

All discharge densities had a limited effect on the total heat release rate and the associated total energy, as almost all combustible material was consumed in the tests. The best reduction of the total energy was achieved in Test 2S(10) and Test 3S(10), i.e., those tests with a water discharge density of 10 mm/min. The least reduction of the total energy was recorded with a discharge density of 5 mm/min, where virtually all combustible material was consumed.

The most efficient reduction of the convective heat release rate and the associated convective energy was demonstrated in Test 3S(10), when discharging 10 mm/min at the higher system operating pressure. The water discharge density of 5 mm/min reduced the convective heat release rate the least of the tested water spray systems.

Somewhat surprisingly, the best cooling of the side plates was experienced in Test 3S(10), despite the fact that it would be expected that the direct cooling would be best with a discharge rate of 15 mm/min. This is an indication that the absorption of the heat radiation, associated with the smaller droplets generated at the higher system operating pressure, combined with a relatively high discharge density is an

effective combination, limiting the risk for fire spread to adjacent vehicles if the direct application of water to the seat of the fire is obscured.

The water discharge density of 5 mm/min is also, in this respect, clearly the worst.

A small leakage of the steel roof was discovered after Test 1S(15) and the test was therefore repeated as Test 5S(15). The leakage appeared along the junction between steel plates used for the roof. The steel plates moved apart during the test and the two longitudinal, parallel gaps that were formed were of the order of a few millimetres in width. Although the test data from Test 1S(15) cannot be used for a direct comparison with the other tests, the reduction of the fire size that was experienced is interesting to note. If the roof of a real vehicle burns through, water from the water spray system will have access to the fire and the performance will be significantly improved even if the leakage area is small.

High-pressure water mist system

Only one test was conducted with the high-pressure water mist system which makes a comparison of the efficiency at different discharge densities impossible.

When comparing the results with the water spray system tests it can be concluded that the water mist system reduced the total energy to a level that was slightly lower than the water spray system discharging at 5 mm/min, to a level that was comparable to the system discharging at 15 mm/min. However, the reduction was not as efficient as the water spray system tests when discharging at 10 mm/min.

The total convective energy was reduced to a level that was significantly less than all water spray system tests which underlines the improved cooling efficiency of the smaller water droplets.

Figure 28 shows a histogram of the maximum one minute average total and convective heat release rates, respectively. Note that the plots include data for Test 5S(15), denoted with (*) where the leakage of the steel roof over the trailer occurred.

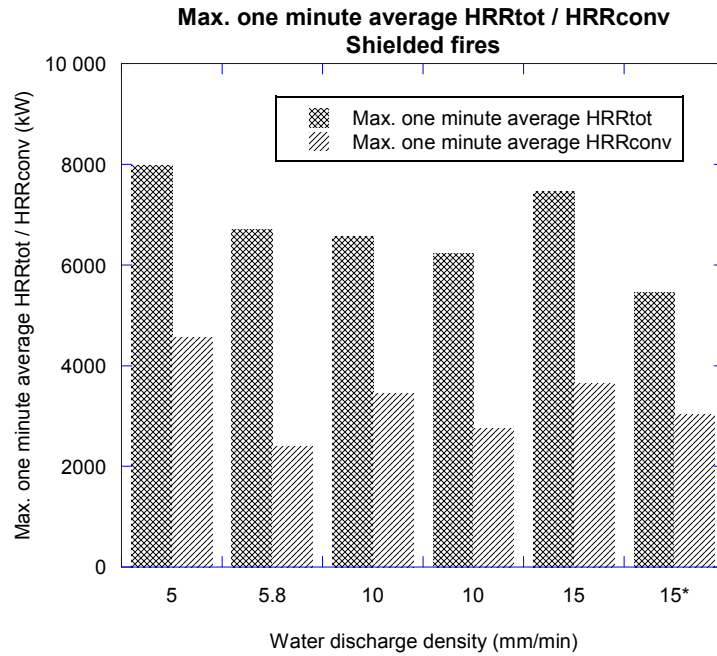


Figure 28 The maximum one minute average total and convective heat release rate for the fire tests with the roof of the trailer mock-up. The (*) indicates the test where the leakage of the steel roof over the trailer occurred.

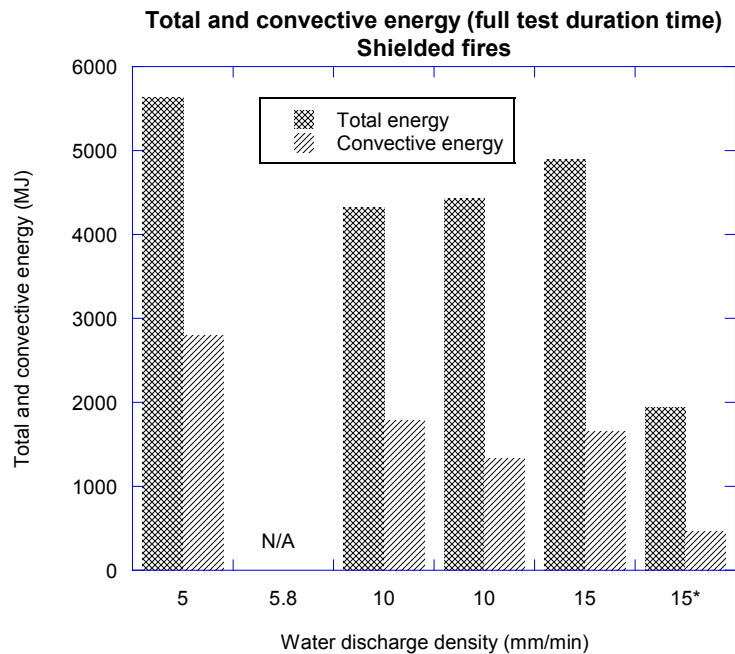


Figure 29 The total and convective energy as a function of the water discharge densities, calculated based on the entire test duration time for the fire tests with the roof of the trailer mock-up. The (*) indicates the test where the leakage of the steel roof over the trailer occurred. No relevant data is available for the high-pressure water mist system (5,8 mm/min) as the test had to be terminated in advance.

Figures 29 and 30 show histograms of the total and convective energy, respectively, over the full test duration time and from fire ignition to 14:00 [min:sec]. Note that the plots include data for Test 5S(15), denoted with (*) where the leakage of the steel roof over the trailer occurred.

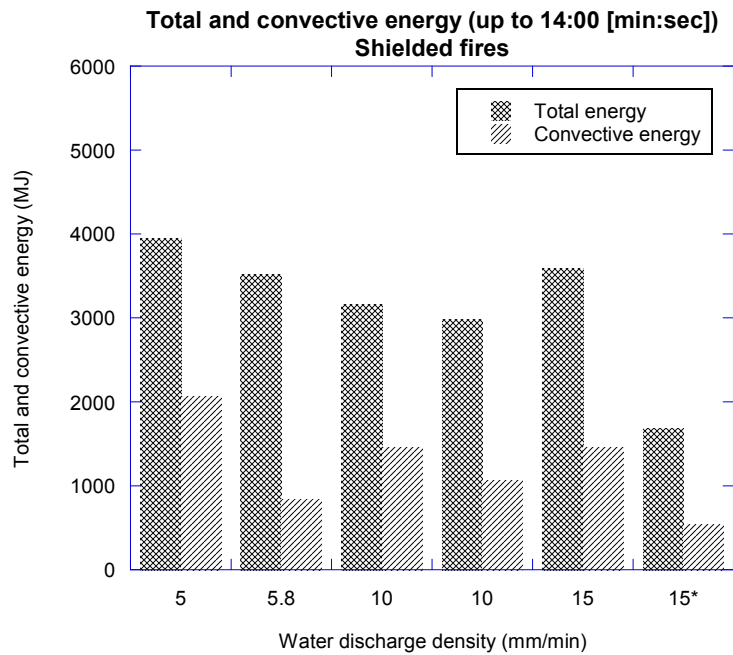


Figure 30 The total and convective energy as a function of the water discharge densities, calculated from fire ignition to 14:00 [min:sec] for the fire tests with the roof of the trailer mock-up. The (*) indicates the test where the leakage of the steel roof over the trailer occurred. Data for the high-pressure water mist system (5,8 mm/min) is included.

The cooling of the steel plates on either sides of the trailer mock-up was not as effective for the high-pressure water mist as the water spray system when discharging 10 mm/min and 15 mm/min, but better than the 5 mm/min discharge density.

7.3 Influence of test methodology

It may be argued that the test set-up, with the measurement of the heat release rate and the ventilation of the fire test hall, creates an environment that is unrealistic, and disadvantageous for the performance of the tested systems, compared to actual conditions on a ro-ro deck.

The maximum upward velocity (just under the mean flame height), u_{0m} , in an axisymmetric buoyant fire plume, similar to a pool fire, can be estimated using the following formula by Heskestad [24]:

$$u_{0m} = 1,97Q^{1/5}$$

For the majority of the tests, the system was manually activated at a convective heat release rate of 3 MW. This heat release rate corresponds to an upward velocity of almost 10 m/s using Heskestad's equation. The centreline velocities tend to have their maxima slightly below the mean flame height and decay to even lower values for higher elevations.

Ingason has investigated fire spread in rack storage, and has developed correlations for in-rack gas temperatures and velocities [25]. Based on model scale and large-scale fire tests, the velocity at the top of a 2,3 m high storage can be estimated to 7 m/s.

These estimations indicate that the measured air velocities generated by the ventilation system (refer to section 2.5) are low compared to the velocities generated in the fire plume. They are therefore judged to have no, or very limited, influence on the test results.

For a water spray or water mist system to successfully suppress a fire in ordinary combustibles, the droplets must be capable of penetrating the fire plume to reach the burning fuel surface. In other words, the total downward momentum of the water spray needs to overcome the upward momentum of the fire plume. Penetration of droplets may also be reduced by the evaporative loss of the smallest droplets as they pass through the fire plume. Although this will tend to cool the flame gases, it will contribute little to the control of a fast-growing fire [26].

In order provide fire suppression, full coverage of the water spray over the burning surfaces is important. For the fire test set-up used in these tests, the coverage between the four central nozzles is important to distribute water towards the central flue spaces of the commodity stacks. Distribution of water on the outside of the stacks of the commodity is also important. Prior to these large-scale tests, water distribution tests were conducted to select the best possible nozzles with a focus on such features [20]. Indeed the nozzles used in the tests may represent the best the market could offer for this specific hazard.

Under actual conditions, the deck above a fire on a ro-ro deck would form a boundary that limits the vertical spread of combustion gases and water vapour. During the tests, most combustion gases and water vapour were ventilated away by the Industrial Calorimeter. This may have been more disadvantageous for the water mist system compared to the water spray system. As previously discussed, the influence of the ventilation conditions on a ro-ro deck has been investigated in model scale [7]. These tests have shown that a fire on a vehicle deck can be very large before it becomes ventilation controlled, due to the large volumes associated with ro-ro cargo decks. This would indicate that a global inerting effect due to build-up of water vapour inside the space could occur at a later stage of the fire. Division of the deck into separate sections could be an efficient way to limit the size of a fire and provide conditions for inerting by combustion products in combination with water vapour at an earlier stage.

8 Conclusions

8.1 The results from the tests

The tests where the fires were fully exposed to the water spray show that there is a clear relationship between the level of performance and the water application rate. A discharge density of 15 mm/min provided immediate fire suppression, 10 mm/min fire suppression, and 5 mm/min fire control. However, improvements in performance were also documented with a higher system operating pressure and associated smaller water droplets.

The high-pressure water mist system provided fire control at a discharge density of 5,8 mm/min. However, tests at 3,75 and 4,6 mm/min, respectively, provided no fire control.

For the fires where the fire was shielded from direct water application, the tested systems had a limited effect on the total heat release rate and the associated total energy, as almost all combustible material was consumed in the tests. The most efficient reduction of the convective heat release rate and the associated convective energy was demonstrated with an application rate of 10 mm/min at a higher system operating pressure.

The tests also prove that if the roof of a real vehicle burns through, water from the water spray system will have access to the fire and the performance will be significantly improved, even if the leakage area is small.

The high-pressure water mist system provided an improved reduction of the convective heat release rate and the associated convective energy as compared to the water spray system. However, no improved reduction of the total heat release rate and the associated total energy, was documented, i.e., the ability to reduce the actual heat release rate was not enhanced.

8.2 Practical implications

A water spray system designed in accordance with IMO Resolution A.123 (V) for vehicle and ro-ro cargo spaces in excess of 2,5 m in height has a water discharge density of 5 mm/min.

This density would provide fire control of a fire in the trailer of a heavy goods vehicle, i.e., the peak heat release rate would be significantly reduced compared to free-burn conditions. However, there is still a non-negligible risk that fire would spread to adjacent vehicles and the heating of the exposed steel deck above the fire is so high that fire spread to other decks is probable.

An increase of the water discharge density to 10 mm/min would drastically improve the performance of the system. A further increase of the density would not improve the performance as much, but would add a further safety factor to the design.

An increase of the system operating pressure would generate smaller water droplets and these tests show that the performance, in terms of fire suppression, heat attenuation and cooling of combustible gases, also improves. However, an increase in the system operating pressure will also result in a decrease in the coverage area of the nozzles, since the spray pattern tends to draw inwards at higher pressures. If the system operating pressure is increased it is, therefore, essential to reduce the coverage area of the individual nozzles, in order to ensure that proper water coverage is provided by the system as a whole. This is especially important for applications where the vertical distance from the nozzles to the protected area is limited, as on vehicle decks.

An increased system operating pressure could also increase the velocities and the mobility of the droplets, but the ability of the droplets to penetrate the fire plume may be reduced due to their lesser size. Care should therefore be given to the maximum installation height in such a system.

Since the beginning of the 1990's, water mist systems have become a viable alternative to traditional sprinkler systems in accommodation spaces and public areas on board ships. For these applications, a selling argument has been the reduced water demands. Water mist systems are also replacing halon in machinery spaces and are used as an alternative to hazardous agents as Carbon Dioxide.

For vehicle and ro-ro cargo spaces, the fire load is virtually enormous and the volume of the spaces is huge. A fire may develop very fast and spread rapidly from vehicle to vehicle, facts that place stringent demands on the system. These tests show that a water mist system may be an alternative to a traditional water spray system. However, the potential savings in water demand seem small, at least for ro-ro decks where the fire load is constituted of freight trucks or other larger vehicles.

References

- 1 Resolution A.123(V), "Recommendation on fixed fire extinguishing systems for special category spaces", International Maritime Organization, London, United Kingdom, October 26, 1967
- 2 Fribert, F., Hansen, G., et al, "Extinction of Fire in Ships by Automatic Sprinkler Systems and Fixed Pressure Water-spraying Systems", Denmark, June 1963
- 3 Arvidson, Magnus, Ingason, Haukur and Persson, Henry, "Water Based Fire Protection Systems for Vehicle Decks on Ro-Ro Passenger Ferries, BRANDFORSK Project 421-941", SP Report 1997:03, Swedish National Testing and Research Institute, 1997
- 4 Arvidson, Magnus, "Large Scale Ro-Ro Vehicle Deck Fire Test, NORDTEST Project 1299-96, BRANDFORSK Project 421-941", SP Report 1997:15, Swedish National Testing and Research Institute, 1997
- 5 Video entitled "Large Scale Ro-Ro Vehicle Deck Fire Test, Conducted at SP on the 23rd of May 1997", Swedish National Testing and Research Institute, Borås, 1997
- 6 Arvidson, Magnus and Torstensson, Håkan, "En förstudie angående vattenbaserade släcksystem för lastutrymmen på fartyg, Brandforsk projekt 511-001", SP Rapport 2002:22 (in Swedish), 2002
- 7 Larsson, Ida, Ingason, Haukur and Arvidson, Magnus, "Model scale fire tests on a vehicle deck on board a ship", SP Report 2002:05, Swedish National Testing and Research Institute, Borås, Sweden, 2002
- 8 Shipp, M., Annable, K. and Williams, C., "Assessment of the Fire Behaviour of Cargo Loaded on Ro-Ro Vehicle Decks in Relation to the Design Standards for Fire Suppression Systems", BRE Fire and Security, Client report number 227974, November 3, 2006.
- 9 FP51/3/2/Rev.1, "Assessment of the fire behaviour of cargo loaded on ro-ro vehicle decks in relation to the design standards for fire extinguishing systems, Submitted by the United Kingdom to IMO Sub-Committee meeting FP51 on Fire Protection, 27 November 2006
- 10 Maccari, Alessandro, "Application of CFD Analysis for Fire Modelling"
- 11 Arvidson, Magnus, Axelsson, Jesper, Simonson, Margaret and Tuovinen, Heimo, "Fire safety approach on the DESSO ROPAX", SP Rapport 2006:01, Swedish National Testing and Research Institute, 2006
- 12 MSC/Circ. 914, "Guidelines for the approval of alternative fixed water-based fire-fighting systems for special category spaces", June 4, 1999

- 13 Arvidson, Magnus and Vaari, Jukka (VTT), "A preparatory study of appropriate fire test procedures for sprinkler systems on ro-ro cargo decks", SP Report 2006:02, 2006
- 14 Vaari, Jukka and Ala-Outinen, Tiina, "Performance requirements for fixed water-based fire fighting systems on shipboard vehicle decks", VTT RESEARCH REPORT No. VTT-S-11913-06, 2006
- 15 Annex 6 of FP51/3/1, "The Report of the correspondence group", Submitted by the United States to IMO Sub-Committee meeting FP51 on Fire Protection, 24 October 2006
- 16 MSC.1/Circ. 1272, "Guidelines for the approval of fixed water-based fire-fighting systems for ro-ro spaces and special category spaces equivalent to that referred to in Resolution A.123(V)", June 4, 2008
- 17 Fires on Ro-Ro decks, DNV Technical Paper, Paper Series No. 2005-P018, September 2005
- 18 FSI 16/6/2, "Information concerning the fire on the ro-ro cargo ship UND ADRIYATIK", document submitted by Croatia and Turkey to the 16th Sub-Committee on Flag State Implementation, March 27, 2008
- 19 Arvidson, Magnus, "Down-scaled fire tests using a trailer mock-up", SP Report 2008:42, SP Technical Research Institute of Sweden, 2008
- 20 Arvidson, Magnus, "Water distribution tests using different water spray nozzles", SP Arbetsrapport 2009:04, SP Technical Research Institute of Sweden, 2009
- 21 Backman, Haide and Nordström, Rolf, "Improved Performance of European Long Haulage Transport", TFK Report 2002:6E, TFK Institutet för transportforskning, 2002
- 22 Arvidson, Magnus and Lönnermark, Anders, "Commodity classification tests of selected ordinary combustible products", SP Report 2002:03, ISBN 91-7848-891-5, 2002
- 23 Bill, Robert G., Stavrianidis, Paraskevas, Hill, Jr, Edward E and Brown, William R, "Water mist fire protection in residential occupancies", FMRC J.I. 0Y1N9.RA, 0Z0J1.RA, Factory Mutual Research, November 1999
- 24 Heskestad, Gunnar, "Fire plumes, Flame Height, and Air Entrainment", The SFPE Handbook of Fire Protection Engineering, Fourth Edition, National Fire Protection Association, 2008
- 25 Ingason, Haukur, "Experimental and Theoretical Study of Rack Storage Fires", Report LUTVDG/(TVBB-1013), 1996

- 26 Drysdale, Dougal, "An introduction to fire dynamics", John Wiley & Sons Ltd, 1985

Photos: Test 1E(15)



Figure A-1 The water spray of the nozzles prior to Test 1E(15).



Figure A-2 Test 1E(15): Photo taken 30 seconds after fire ignition.



Figure A-3 Test 1E(15): Photo taken 01:00 [min:sec] after fire ignition.



Figure A-4 Test 1E(15): Photo taken 01:30 [min:sec] after fire ignition. The top surface of the commodity has started to become involved in the fire.



Figure A-5 Test 1E(15): Photo taken 02:00 [min:sec], at the moment the water spray system was manually activated. The fire has reached a convective heat release rate of 3000 kW and a total heat release rate of approximately 5000 kW.



Figure A-6 Test 1E(15): Photo taken 02:30 [min:sec] after fire ignition. The fire is suppressed and flames are concentrated to the longitudinal flue space and the horizontal area between the pallet loads forming the central stack.



Figure A-7 Test 1E(15): Photo taken 03:00 [min:sec] after fire ignition. The fire is suppressed and only small flames are visible at the longitudinal and vertical flue spaces.



Figure A-8 Test 1E(15): The initiation of manual fire fighting 10:00 [min:sec] after fire ignition.



Figure A-9 Test 1E(15): Manual fire fighting of the remaining fire after the test. Note that the outer stacks of commodity have been removed in order to increase the access to the remaining (very small) fire.



Figure A-10 Test 1E(15): Manual fire fighting of the remaining fire after the test. Note that the outer stacks of commodity have been removed in order to increase the access to the remaining (very small) fire.

Photos: Test 2E(10)



Figure A-11 Test 2E(10): Photo taken 30 seconds after fire ignition.



Figure A-12 Test 2E(10): Photo taken 01:00 [min:sec] after fire ignition.



Figure A-13 Test 2E(10): Photo taken 01:30 [min:sec] after fire ignition.



Figure A-14 Test 2E(10): Photo taken 02:00 [min:sec] after fire ignition.



Figure A-15 Test 2E(10): Photo taken at 02:10 [min:sec], moments after the water spray system was manually activated.



Figure A-16 Test 2E(10): The fire size at moments after the water spray system was manually activated, as seen from floor level.



Figure A-17 Test 2E(10): Photo taken 02:30 [min:sec] after fire ignition. The fire size is controlled and flames are concentrated to the longitudinal flue space and the horizontal area between the pallet loads forming the central stack.



Figure A-18 Test 2E(10): Photo taken 03:00 [min:sec] after fire ignition. The fire size is controlled and flames are concentrated to the longitudinal flue space and the horizontal area between the pallet loads forming the central stack.



Figure A-19 Test 2E(10): Photo taken 03:30 [min:sec] after fire ignition. The fire size is controlled and flames are concentrated to the longitudinal flue space and the horizontal area between the pallet loads forming the central stack.



Figure A-20 Test 2E(10): Photo taken 03:30 [min:sec] after fire ignition as seen from a floor level.



Figure A-21 Test 2E(10): Fire damages, as seen from the left hand side.



Figure A-22 Test 2E(10): Fire damages, as seen from the right hand side.

Photos: Test 3E(10)



Figure A-23 Test 3E(10): Photo taken 30 seconds after fire ignition.



Figure A-24 Test 3E(10): Photo taken 01:00 [min:sec] after fire ignition.



Figure A-25 Test 3E(10): Photo taken 01:30 [min:sec] after fire ignition.



Figure A-26 Test 3E(10): Photo taken at the moment the water spray system was manually activated, 02:00 [min:sec] after fire ignition.



Figure A-27 Test 3E(10): Photo taken 02:30 [min:sec] after fire ignition.



Figure A-28 Test 3E(10): Photo taken 03:00 [min:sec] after fire ignition.



Figure A-29 Test 3E(10): Photo taken 03:30 [min:sec] after fire ignition.



Figure A-30 Test 3E(10): Photo taken 04:00 [min:sec] after fire ignition. The test set-up is obscured by smoke.



Figure A-31 Test 3E(10): Fire damages as seen from the left hand side.



Figure A-32 Test 3E(10): Fire damages as seen from the right hand side.

Photos: Test 4E(5)



Figure A-33 Test 4E(5): Photo taken 30 seconds after fire ignition.



Figure A-34 Test 4E(5): Photo taken 01:00 [min:sec] after fire ignition.



Figure A-35 Test 4E(5): Photo taken 01:30 [min:sec] after fire ignition.



Figure A-36 Test 4E(5): Photo taken at the moment the water spray system was manually activated, 01:58 [min:sec] after fire ignition.



Figure A-37 Test 4E(5): Photo taken 02:30 [min:sec] after fire ignition.



Figure A-38 Test 4E(5): Photo taken 03:00 [min:sec] after fire ignition.



Figure A-39 Test 4E(5): Photo taken 03:30 [min:sec] after fire ignition.



Figure A-40 Test 4E(5): Photo taken 04:00 [min:sec] after fire ignition.



Figure A-41 Test 4E(5): Photo taken 04:30 [min:sec] after fire ignition.



Figure A-42 Test 4E(5): Photo taken 05:00 [min:sec] after fire ignition.



Figure A-43 Test 4E(5): Photo taken 05:30 [min:sec] after fire ignition.



Figure A-44 Test 4E(5): Photo taken 06:00 [min:sec] after fire ignition.



Figure A-45 Test 4E(5): Photo taken 07:00 [min:sec] after fire ignition.



Figure A-46 Test 4E(5): Photo taken 07:00 [min:sec] after fire ignition as seen from floor level.



Figure A-47 Test 4E(5): Photo taken 10:00 [min:sec] after fire ignition as seen from floor level.



Figure A-48 Test 4E(5): Photo taken 14:30 [min:sec] after fire ignition.



Figure A-49 Test 4E(5): Fire damages as seen from the right hand side.



Figure A-50 Test 4E(5): Fire damages as seen from the left hand side.



Figure A-51 Test 4E(5): Fire damages as seen from the front short side.

Photos: Test 5E(HP-3,75)



Figure A-52 Test 5E(HP-3,75): Photo taken 30 seconds after fire ignition.



Figure A-53 Test 5E(HP-3,75): Photo taken 01:00 [min:sec] after fire ignition.



Figure A-54 Test 5E(HP-3,75): Photo taken 01:30 [min:sec] after fire ignition.



Figure A-55 Test 5E(HP-3,75): Photo taken at the moment the high-pressure water mist system was manually activated, 01:58 [min:sec] after fire ignition.



Figure A-56 Test 5E(HP-3,75): Photo taken at 02:30 [min:sec] after fire ignition.



Figure A-57 Test 5E(HP-3,75): Photo taken 05:00 [min:sec] after fire ignition. The fire is not controlled by the system.



Figure A-58 Test 5E(HP-3,75): Photo taken 05:30 [min:sec] after fire ignition, from a different angle. The fire is not controlled by the system and the test is terminated.



Figure A-59 Test 5E(HP-3,75): The fire damages, as seen from the right hand side.



Figure A-60 Test 5E(HP-3,75): The fire damages, as seen from the left hand side.

Photos: Test 6E(HP-4.6)



Figure A-61 Test 6E(HP-4.6): Photo taken 30 seconds after fire ignition.



Figure A-62 Test 6E(HP-4.6): Photo taken 01:00 [min:sec] after fire ignition.



Figure A-63 Test 6E(HP-4.6): Photo taken 01:30 [min:sec] after fire ignition.



Figure A-64 Test 6E(HP-4.6): Photo at about 01:40 [min:sec] after fire ignition, a few seconds prior to the manual activation of the high-pressure water mist system.



Figure A-65 Test 6E(HP-4.6): Photo at 01:45 [min:sec] after fire ignition, at the manual activation of the high-pressure water mist system.



Figure A-66 Test 6E(HP-4.6): Photo at 01:50 [min:sec] after fire ignition, at full system operating pressure of the high-pressure water mist system.



Figure A-67 Test 6E(HP-4.6): Photo at 04:50 [min:sec] after fire ignition, the fire increases in size. The fire is not controlled by the system and the test is terminated.



Figure A-68 Test 6E(HP-4.6): The fire damages, as seen from the right hand side.



Figure A-69 Test 6E(HP-4.6): The fire damages, as seen from the left hand side.

Photos: Test 7E(HP-5.8)



Figure A-70 Test 7E(HP-5.8): Photo taken 30 seconds after fire ignition.



Figure A-71 Test 7E(HP-5.8): Photo taken 01:00 [min:sec] after fire ignition.



Figure A-72 Test 7E(HP-5.8): Photo taken 01:30 [min:sec] after fire ignition.



Figure A-73 Test 7E(HP-5.8): Photo taken 02:04 [min:sec] after fire ignition, at the manual activation of the high-pressure water mist system.



Figure A-74 Test 7E(HP-5.8): Photo taken at approximately 02:06 [min:sec] after fire ignition, soon after the manual activation of the high-pressure water mist system.



Figure A-75 Test 7E(HP-5.8): Photo taken 02:30 [min:sec] after fire ignition.



Figure A-76 Test 7E(HP-5.8): Photo taken 05:00 [min:sec] after fire ignition.



Figure A-77 Test 7E(HP-5.8): Photo taken 30:15 [min:sec] after fire ignition. The high-pressure water mist system has been shut off and manual fire fighting of the remaining (small) fire has started.



Figure A-78 Test 7E(HP-5.8): The fire damages, as seen from the back.



Figure A-79 Test 7E(HP-5.8): The fire damages, as seen from the left hand side, during the removal of the fire damaged pallet loads of commodity at the back end.



Figure A-80 Test 7E(HP-5.8): The fire damages, as seen from the left hand side, after the removal of the fire damaged pallet loads of commodity at the back end.

Photos: Test 8E(10)



Figure A- 81 Test 8E(10): The water spray from the nozzles prior to the test.



Figure A-82 Test 8E(10): Photo taken 30 seconds after fire ignition.



Figure A-83 Test 8E(10): Photo taken 01:00 [min:sec] after fire ignition.



Figure A-84 Test 8E(10): Photo taken 01:30 [min:sec] after fire ignition.



Figure A-85 Test 8E(10): Photo taken 02:00 [min:sec] after fire ignition.



Figure A-86 Test 8E(10): Photo taken 02:30 [min:sec] after fire ignition.



Figure A-87 Test 8E(10): Photo taken 02:33 [min:sec] after fire ignition, at the manual activation of the water spray system.



Figure A- 88 Test 8E(10): Photo taken 02:33 [min:sec] after fire ignition, at the manual activation of the water spray system as seen from floor level.



Figure A-89 Test 8E(10): Photo taken 03:00 [min:sec] after fire ignition.



Figure A-90 Test 8E(10): Photo taken 03:30 [min:sec] after fire ignition.



Figure A-91 Test 8E(10): Photo taken 04:00 [min:sec] after fire ignition.



Figure A-92 Test 8E(10): Photo taken 04:30 [min:sec] after fire ignition.



Figure A-93 Test 8E(10): Photo taken at approximately 04:30 [min:sec] after fire ignition as seen from floor level.



Figure A-94 Test 8E(10): Photo taken 30:15 [min:sec] after fire ignition. The water spray system has been shut off and manual fire fighting of the remaining (small) fire has started.



Figure A-95 Test 8E(10): Fire damages as seen from the back.



Figure A-96 Test 8E(10): Fire damages as seen from the right hand side.

Photos: Test 1S(15)



Figure A-97 Test 1S(15): The water sprays from the nozzles prior the test.



Figure A-98 Test 1S(15): Photo taken 30 seconds after fire ignition.



Figure A-99 Test 1S(15): Photo taken 01:00 [min:sec] after fire ignition.



Figure A-100 Test 1S(15): Photo taken 01:30 [min:sec] after fire ignition.



Figure A-101 Test 1S(15): Photo taken 02:00 [min:sec] after fire ignition.



Figure A-102 Test 1S(15): Photo taken 02:30 [min:sec] after fire ignition.



Figure A-103 Test 1S(15): Photo taken 02:45 [min:sec] after fire ignition, a few seconds after the manual activation of the system.



Figure A-104 Test 1S(15): Photo taken 03:30 [min:sec] after fire ignition.



Figure A-105 Test 1S(15): Fire damages as seen from the right hand side.



Figure A-106 Test 1S(15): Fire damages as seen from the left hand side.

Photos: Test 2S(10)



Figure A-107 Test 2S(10): Photo taken 30 seconds after fire ignition.



Figure A-108 Test 2S(10): Photo taken at 01:00 [min:sec] after fire ignition.



Figure A-109 Test 2S(10): Photo taken at 01:30 [min:sec] after fire ignition.



Figure A-110 Test 2S(10): Photo taken at 02:00 [min:sec] after fire ignition.



Figure A-111 Test 2S(10): Photo taken at 02:12 [min:sec] after fire ignition, at the moment the water spray system was manually activated.



Figure A-112 Test 2S(10): Photo taken at 03:00 [min:sec] after fire ignition.



Figure A-113 Test 2S(10): Photo taken at 06:00 [min:sec] after fire ignition.



Figure A-114 Test 2S(10): Photo taken at 20:00 [min:sec] after fire ignition. The upper pallet loads have been consumed in the fire.



Figure A-115 Test 2S(10): Photo taken at 30:15 [min:sec] after fire ignition. The water spray system has been shut off and manual fire fighting has started.



Figure A-116 Test 2S(10): The fire damages, as seen from the left hand side.



Figure A-117 Test 2S(10): The fire damages as seen from the back.

Photos: Test 3S(10)



Figure A-118 Test 3S(10): The water spray prior to the test.



Figure A-119 Test 3S(10): Photo taken 30 seconds after fire ignition.



Figure A-120 Test 3S(10): Photo taken 01:00 [min:sec] after fire ignition.



Figure A-121 Test 3S(10): Photo taken 01:30 [min:sec] after fire ignition.



Figure A-122 Test 3S(10): Photo taken 02:00 [min:sec] after fire ignition.



Figure A-123 Test 3S(10): Photo taken at 02:29 [min:sec] after fire ignition, at the moment the water spray system was manually activated.



Figure A-124 Test 3S(10): Photo taken 03:00 [min:sec] after fire ignition.



Figure A-125 Test 3S(10): Photo taken 13:00 [min:sec] after fire ignition.



Figure A-126 Test 3S(10): Photo taken at 30:15 [min:sec] after fire ignition. The water spray system has been shut off and manual fire fighting has started.



Figure A-127 Test 3S(10): Fire damages as seen from the back.



Figure A-128 Test 3S(10): Fire damages as seen from the left hand side.

Photos: Test 4S(5)



Figure A-129 Test 4S(5): Photo taken 30 seconds after fire ignition.



Figure A-130 Test 4S(5): Photo taken 01:00 [min:sec] after fire ignition.



Figure A-131 Test 4S(5): Photo taken 01:30 [min:sec] after fire ignition.



Figure A-132 Test 4S(5): Photo taken 02:00 [min:sec] after fire ignition.



Figure A-133 Test 4S(5): Photo taken at 02:25 [min:sec] after fire ignition, at the moment the water spray system was manually activated.



Figure A-134 Test 4S(5): Photo taken 03:00 [min:sec] after fire ignition.



Figure A-135 Test 4S(5): Photo taken 05:00 [min:sec] after fire ignition, from another angle.



Figure A-136 Test 4S(5): Photo taken 08:00 [min:sec] after fire ignition.



Figure A-137 Test 4S(5): Photo taken 13:00 [min:sec] after fire ignition.



Figure A-138 Test 4S(5): Photo taken 18:00 [min:sec] after fire ignition.



Figure A-139 Test 4S(5): Photo taken 30:15 [min:sec] after fire ignition. The water spray system has been shut off and manual fire fighting has started.



Figure A-140 Test 4S(5): The fire damages after the test. Almost all combustible material is consumed.

Photos: Test 5S(15)



Figure A-141 Test 5S(15): Photo taken 30 seconds after fire ignition.



Figure A-142 Test 5S(15): Photo taken 01:00 [min:sec] after fire ignition.



Figure A-143 Test 5S(15): Photo taken 01:30 [min:sec] after fire ignition.



Figure A-144 Test 5S(15): Photo taken 02:00 [min:sec] after fire ignition



Figure A-145 Test 5S(15): Photo taken 02:13 [min:sec] after fire ignition, at the moment the water spray system was manually activated.



Figure A-146 Test 5S(15): Photo taken 03:00 [min:sec] after fire ignition.



Figure A-147 Test 5S(15): Photo taken 08:00 [min:sec] after fire ignition.



Figure A-148 Test 5S(15): Photo taken 20:00 [min:sec] after fire ignition.



Figure A-149 Test 5S(15): Photo taken 30:15 [min:sec] after fire ignition. The water spray system has been shut off and manual fire fighting has started.



Figure A-150 Test 5S(15): The fire damages, as seen from left hand side.



Figure A-151 Test 5S(15): The fire damages, as seen from back.

Photos: Test 6S(HP-5.8)



Figure A-152 Test 6S(HP-5.8): Photo taken 30 seconds after fire ignition.



Figure A-153 Test 6S(HP-5.8): Photo taken 01:00 [min:sec] after fire ignition.



Figure A-154 Test 6S(HP-5.8): Photo taken 01:30 [min:sec] after fire ignition.



Figure A-155 Test 6S(HP-5.8): Photo taken 02:00 [min:sec] after fire ignition.



Figure A-156 Test 6S(HP-5.8): Photo taken 02:35 [min:sec] after fire ignition, at the moment the high-pressure water mist system was manually activated.



Figure A-157 Test 6S(HP-5.8): Photo taken 03:00 [min:sec] after fire ignition. The visibility is obscured by the water spray.



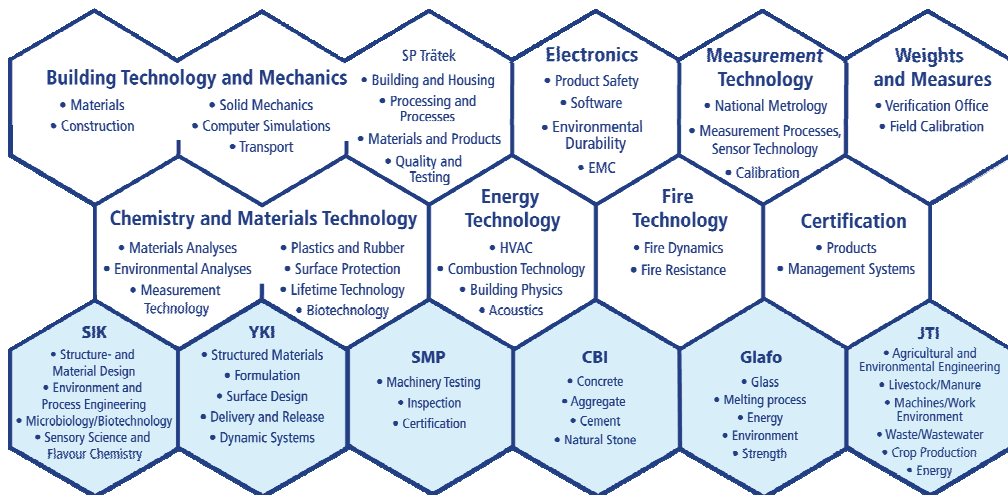
Figure A-158 Test 6S(HP-5.8): Photo taken 16:20 [min:sec] after fire ignition, when the manual fire fighting was initiated.



Figure A-159 Test 6S(HP-5.8): Fire damages as seen from the left hand side.

SP Technical Research Institute of Sweden develops and transfers technology for improving competitiveness and quality in industry, and for safety, conservation of resources and good environment in society as a whole. With Sweden's widest and most sophisticated range of equipment and expertise for technical investigation, measurement, testing and certification, we perform research and development in close liaison with universities, institutes of technology and international partners.

SP is a EU-notified body and accredited test laboratory. Our headquarters are in Borås, in the west part of Sweden.



SP consists of eight technology units and six subsidiary companies. Three of the companies, CBI, Glafo and JTI are each 60 % owned by SP and 40 % by their respective industries.



SP Technical Research Institute of Sweden

Box 857, SE-501 15 BORÅS, SWEDEN

Telephone: +46 10 516 50 00, Telefax: +46 33 13 55 02

E-mail: info@sp.se, Internet: www.sp.se

www.sp.se

Fire Technology

SP Report 2009:29

ISBN 978-91-86319-17-5

ISSN 0284-5172